DOCKING MECHANISM FOR AN AMBULATORY MICROROBOT

A Thesis

Presented to the Faculty of the Graduate School

of Cornell University

in Partial Fulfillment of the Requirements for the Degree of

Masters of Science

by

Chaitanya Dasari

May 2023

ABSTRACT

Ambulatory locomotion in nature has evolved to address major challenges, such as varying contact dynamics, harsh unstructured terrains, and power limitations. This has been an inspiration for engineers and scientists to develop a novel class of bio-inspired robots such as HAMR and RoACH. A major hindrance in the practical application of these robots is the inability to traverse across unstructured terrain and limited payload capacity. Insects work collaboratively to carry objects that are significantly larger than their body mass and build structures (i.e., bridges or rafts) to traverse over obstacles, creating physical connections and chain-like structures to achieve these tasks. Modular robots at conventional scales have demonstrated a number of attachment strategies, but many cannot be employed on the mm scale due to the physics of scaling. Here we address this challenge by developing a docking mechanism that meets the size, weight, and power requirements for a cm-scale ambulatory microrobot that enables the formation of chain-like structures. In this work, we discuss the design, manufacturing, and analysis of this docking mechanism, which employs a custom-made low-voltage electromagnetic actuator, a planar spring, and a permanent magnet to achieve mechanical locking between the robots. The actuator runs on less than 2V, consumes 95mW of power, and can generate displacements up to 1 mm. We anticipate our work to be a starting point for more sophisticated modular and swarm ambulatory microrobotic systems.

BIOGRAPHICAL SKETCH

Chaitanya Dasari was born in Rajahmundry, a city on the eastern banks of the sacred Godavari River, in the southeast Indian state of Andhra Pradesh. An unwavering love for Physics and Mathematics coupled with a penchant for solving complicated problems in high school made him choose the path of mechanical engineering. He did his undergraduate studies at the Indian Institute of Technology, Bhubaneswar, where he developed a passion for fluid mechanics and applied mathematics. He graduated in 2019 and moved on to pursue research at the Indian Institute of Science. During his time and interaction with professors at IISc led to an interest in pursuing a Master's at Cornell University. At Cornell, he developed an interest in robotics. He resonated with the research by Prof. Elizabeth Farrell Helbling, who works on centimeter-scale robots.

Besides academics, Chaitanya was actively involved in Cornell India Association, Indian graduate student organization, and served as Treasurer.

This document is dedicated to all Cornell graduate students.

ACKNOWLEDGEMENTS

I would like to express my gratitude and appreciation to several individuals who have supported and contributed to the successful completion of this thesis. First and foremost, I am deeply indebted to my principal advisor, Professor Elizabeth Farrell Helbling, for her invaluable guidance, encouragement, and mentorship throughout this journey. Her insightful feedback and unwavering support have been instrumental in shaping my research and personal growth.

I would also like to thank my committee member, Professor Tapomayukh Bhattacharjee, for his valuable insights and suggestions that have helped me refine my research and presentation.

My heartfelt thanks go to my friends Harish, Ivan, Shashank, Rishi, Sunitha and Swatah, for their unwavering support, encouragement, and motivation during the ups and downs of this academic journey. Their invaluable friendship and companionship have made the long hours of work more bearable and enjoyable.

I would also like to acknowledge my fellow Master's students in the MAE program, who have been a source of inspiration and motivation throughout my academic journey. Their insightful discussions, collaborative efforts, and support have enriched my learning experience and made my time in the program more fulfilling. I am grateful for their camaraderie and the memories we have shared together.

Finally, I would like to acknowledge the support and understanding of my family throughout my academic journey. Their unwavering support and encouragement have been the cornerstone of my success, and for that, I will always be grateful.

TABLE OF CONTENTS

LIST OF TABLES

LIST OF FIGURES

CHAPTER 1

INTRODUCTION

1.1 Bioinspiration

Nature has evolved to survive in extreme environments. Bio-inspired robotics attempts to translate biological principles into engineered systems. Understanding the principles of movement found in nature initiates the design of bio-inspired robots. Engineered systems at the conventional scale provide a diverse range of transportation modes on the ground, air, and water, with the capability to transport huge payloads across long distances in the shortest time or with the least energy consumption. In contrast, locomotion in nature is primarily for survival. Each species uses its own mode of locomotion to hunt for food, find mates, and escape danger. Therefore, the demands for biological locomotion are more complicated than human transport systems resulting in very diverse biological locomotion mechanisms. For example, legs of different numbers, and sizes; humans are bipedal, many reptiles are quadrupeds, and insects are hexapods. Wings of different shapes and impedance; birds, bats, and flying insects flap their wings to generate lift. Snakes and worms move by creating waves in their body.

In addition to individual locomotion strategies, nature also provides examples of communication and coordination among individuals in a collective. Fire ants are known for their ability to form rafts (Fig. 1.3) to escape flooding [29]. When their underground nests are flooded, the ants link their bodies together and form a buoyant raft on the water's surface. They use their bodies to trap air and create pockets of air within the raft, allowing them to float and stay afloat

Figure 1.1: Chain of weaver ants folds over the tip of a leaf during the construction of the arboreal nest, a remarkable example of cooperative behavior. The workers shorten the chains by climbing up on the backs of nestmates while hauling the edge of the leaf behind them. [19]

for extended periods. Asian honey bees exhibit balling behavior (Fig. 1.2) to defend their colony against hornets by forming a tight ball around the intruder, generating heat to increase the temperature within the ball and effectively kill the hornet due to the honey bees' higher tolerance to heat [53]. This behavior is observed in species such as Apis cerana and Apis dorsata as a defense mechanism against hornet attacks. The formation of bridges and chains have been reported in the army ant Eciton [61], the African weaver ant Oecophylla longinoda [23], or the honeybee Apis mellifica [8]: workers form bridges or chains by linking their bodies when they explore a new space, create a bivouac, or cooperate in nest building allowing them to survive harsh conditions, carry heavy prey, and traverse harsh unstructured terrains as seen in Fig 1.1.

The pulling chain style aggregation[2] is observed in weaver ants, named for their nest construction abilities. When a leaf is broader than the length of an ant's body, or when two leaves must be pulled together across a wide space, the

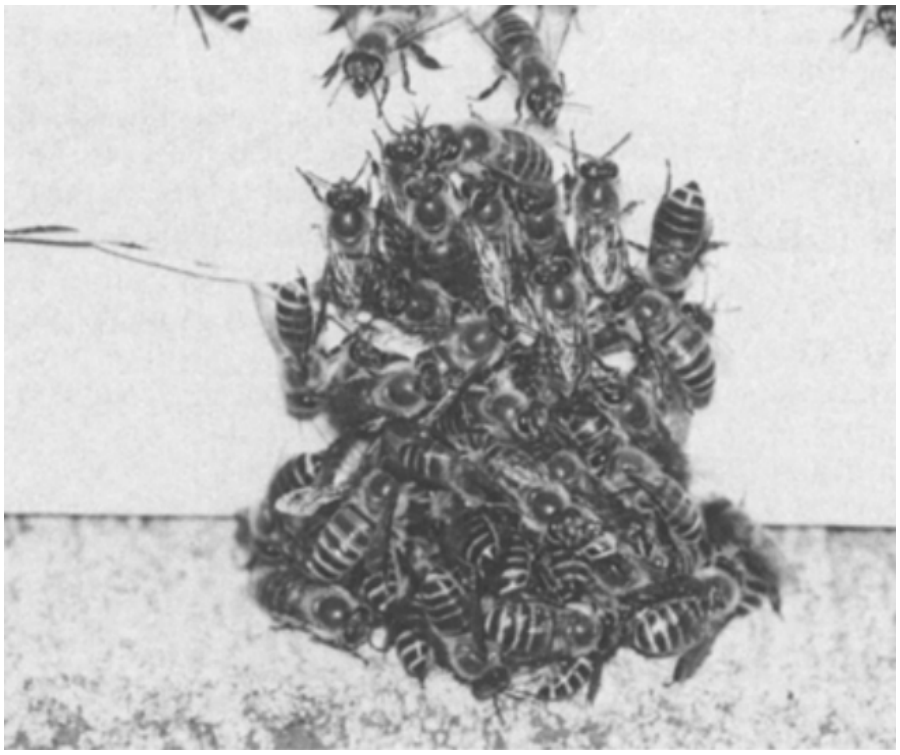

Figure 1.2: A ball of around 250 worker honeybees captures a hornet at the hive entrance, with the internal temperature of the ball being monitored using a micro thermistor.[53]

Figure 1.3: Red imported fire ant colony floating in flood water. ©Bart D. Drees, Texas Fire Ant Project Coordinator

workers form living bridges between the points to be joined. Additional ants in the chain climb onto the backs of their neighbors and pull backward, thus shortening the chain and bringing the leaf edges together.

1.2 Bio-inspired robots

An improved understanding of insect locomotion [13] has enabled the creation of multiple insect-scale legged robots. Inspiration from multi-legged insects especially the cockroach has led to the development of DASH[7], RoACH [25], DyanoRoACH[24], OctoRoACH[56], HAMR[4], and a crawling robot [60] which utilize the alternating tripod gait seen in hexapods. Multilegged robots that are modeled after centipedes and use various tripod gaits have also been designed[22].

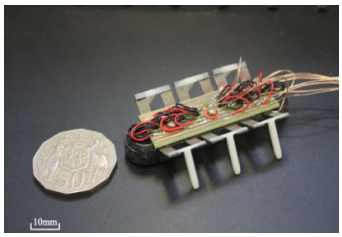

(a) MinRAR V1 [57]

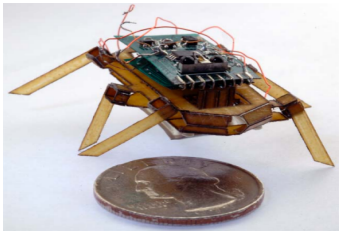

(b) RoACH [25]

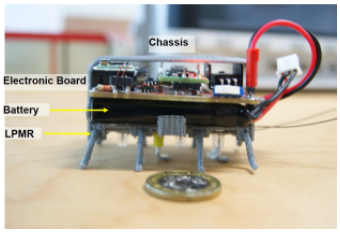

(c) LPMR [20]

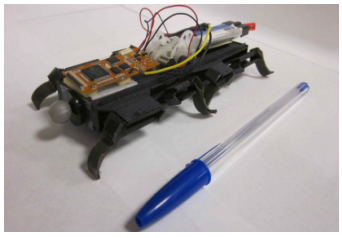

(d) OctoRoach [56]

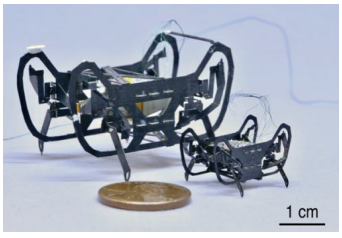

(e) HAMR-VI and HAMR-Jr [30]

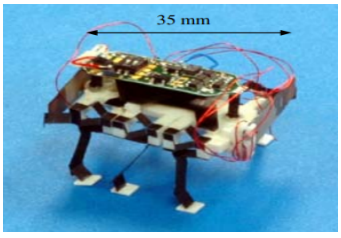

(f) Crawler [60]

Figure 1.4: Ambulatory microrobots at the centimeter scale.

Robot	Mass	Length	Speed (BL/s)	Power	Payload
MinRAR V1 [57]	16 g	55mm	9.45	2.48W	-
HAMR-Jr [30]	320 mg	22.5mm	13.9	21 mW	3.2g
LPMR [20]	6.27 g	50 mm	6	0.22 W	100g
DASH [7]	16.2 g	10 cm	15		
Roach [25]	2.4 g	30 mm	1	1.66 W	-

Table 1.1: Characteristics of centimeter scale ambulatory microrobots

1.3 Motivation

Taking inspiration from nature, in order to enhance obstacle traversal and increase payload capacity in microrobots, this study looks at the design and manufacture of attachment mechanisms to create chain-like structures in microrobots.

A major hindrance in the practical application of microrobots is the ability to traverse across unstructured terrains. A chain-like structure would enable the microrobot to traverse across gaps greater than one bodylength. Also, it increases the payload capacity enabling longer working time and increased capacity to accommodate multiple sensors. The benefits of forming chain-like morphologies have been demonstrated and proved by several mesoscale modular robotic systems. SMORES-EP (Self-Assembly Modular Robot for Extreme Shape-shifting)[68] developed at the University of Pennsylvania is a modular robot each of the size of an 80mm cube. Each module has four rotational degree-of-freedom with four connectors faces, giving it the ability to form complex configurations drastically increasing its capability to perform a large variety of manipulation and locomotion tasks [44, 33]. Fig. 1.5(a) shows seven SMORES-EP modules assemble in a snake-like configuration in order to climb a table of 3 module lengths high. Ozkan et al., demonstrate the improvement in obstacle

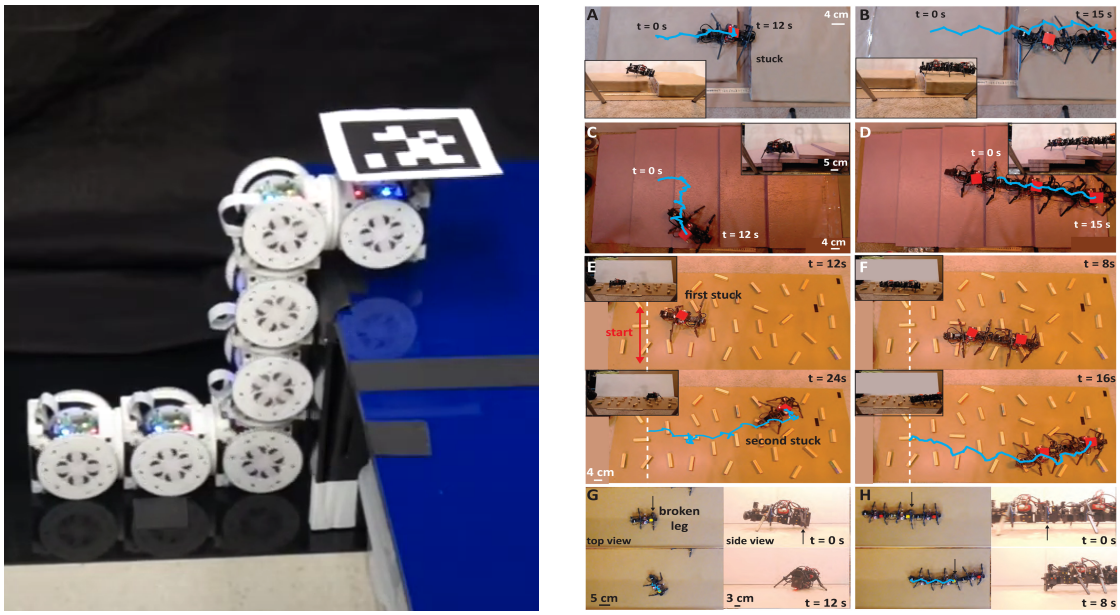

(a) SMORES-EP (b) Modular legged robot

Figure 1.5: Meso-scale modular robotic systems demonstrating obstacle traversal and increased payload [32, 54] (a) The SMORES-EP modules form a seven-module length chain-like structure to climb a table of three module lengths high. (b) Comparison of the locomotion abilities of single and multi quadruped robots in a variety of difficult situations, gaps, stairs, and rough terrain with obstacles

navigation capabilities [54] of quadruped robots when forming chain-like structures. The quadruped robot designed for the study is 22 cm long and weighs 350 g. The robot is actuated using servos and employs a magnetic connection mechanism. Fig. 1.5(b) contrasts the obstacle traversal capabilities, by replicating complex terrain in a lab setup, of a single quadruped robot against 2 or 3 chained robots.

1.4 Project definition and Design Parameters

In order to enhance obstacle traversal and increase payload capacity in micro-robots, this study looks at the design and manufacture of attachment mecha-

nisms to create chain-like structures in microrobots. The goal is to develop a docking mechanism for a sub-gram ambulatory microrobot. As demonstrated by similarly sized robotic vehicles, these systems can carry approximately 3 grams without compromising performance. We thus restrict the mechanism weight at 150 mg (5% of maximum payload) to allow for control autonomy and sensing for future applications. We target a characteristic length of 10 mm, approximately 33% the typical bodylength of a sub-gram ambulatory microrobot.

1.5 Thesis organization

- Chapter 2 provides an overview of common attachment strategies used in modular robots, examining their advantages and limitations. The chapter also surveys various types of actuators that are suitable for cm-scale robots, with a focus on selecting the most appropriate actuation method for the mechanism being discussed. This chapter serves to highlight the attachment strategies and actuator options available for cm-scale robots, considering their benefits and drawbacks in the context of our mechanism.
- Chapter 3 presents the coupling mechanism for an ambulatory microrobot, which utilizes a custom linear electromagnetic actuator along with a pin lock mechanism to form a robust attachment. To simplify the manufacturing process, we designed a planar spiral spring. This work represents the first coupling mechanism for an ambulatory microrobot.
- Chapter 4 discusses the integration of power and control electronics for our mechanism. As the electronics were not implemented at the cm scale, we utilize an H-bridge motor driver and Arduino to send control signals

to the electromagnetic actuator. This chapter delves into the details of how we successfully incorporated the necessary electronics to enable effective control and operation of our mechanism.

- Chapter 5 showcases the results of various experiments conducted to validate the stiffness of the spring, the performance of the linear electromagnetic actuator design, and the loading capacity of the mechanism. In this section, we provide a comprehensive analysis of the experimental findings, including data, graphs, and observations, to verify the effectiveness and functionality of our mechanism's key components.
- Finally, we conclude with a discussion on the further steps for integration of the proposed docking mechanism into an ambulatory microrobot, extensive mechanical testing, at-scale electronics, and autonomous docking. Additionally, we discuss the potential scope for improvement of the docking mechanism.

CHAPTER 2

ATTACHMENT AND ACTUATION STRATEGIES IN ROBOTS

The attachment strategy is a critical aspect of modular robotic systems, as it determines the overall functionality and performance of the system. In this chapter, we delve into the crucial aspect of attachment strategies in modular robotic systems, with a specific focus on their performance at the centimeter (cm) scale. We examine various commonly used attachment strategies, evaluating their advantages and disadvantages, as well as their suitability for cm-scale applications. The goal is to identify the best attachment strategy for the mechanism being designed in this work. Additionally, we explore the different actuation options in bio-inspired cm-scale robots, taking into consideration factors such as size, range of motion, speed, precision, resolution, power consumption, durability, and cost-effectiveness. This comprehensive evaluation will help us determine the most suitable actuation option that complements the chosen attachment strategy for our mechanism.

2.1 Attachment strategies in robots

There are a number of attachment strategies currently employed in cm-scale robotic systems: ranging from electromechanical, magnetic, electrostatic, and electromagnetic, to passive. Initially, modular robotic systems relied on magnetic and electromagnetic couplings due to their simplicity and reliability. These coupling mechanisms were ideal for early modular robotic systems that had limited computational power and sensory capabilities, as they did not require complex sensors or algorithms to establish a connection [15]. However, with the advent of inexpensive sensors, novel actuators, and intelligent design, there has

Name	Type	Actuation	Size(mm)
XBot [12]	Perm.Mag	SMA	
MTRAN-III [49]	Hooks	DC motor	65 X 65 X 130
Roombots [63]	Hooks	DC motor	220 X 110 X 110
ModRED [3]	Latch	Solenoid	368 X 114 X 1190
Pebbles [14]	Electro.Perm.Mag	Current pulse	12 X 12 X 12
THOR [64]	Perm.Mag	–	ϕ70 X 5
GENFA [12]	Electro.Perm.Mag	DC motor	50 X 40 X 15
M3 Express [72]	Perm.Mag	DC motor	
SMORES [9]	Perm.Mag	DC motor	
CoSMO [43]	Key-Lock	DC motor	100 X 100 X 90
M-Blocks [59]	Perm.Mag	–	105 X 105 X 105
Soldercubes [51]	Binder mat	Heat	

Table 2.1: Features of docking in modular robots

been a shift towards more compact and energy-efficient alternatives.

Today, magnetic and electromechanical docking mechanisms are the preferred choice for the majority of current modular robotic systems. These mechanisms offer a high degree of precision and control, making them ideal for complex tasks. Additionally, they can be easily integrated with advanced sensing and control systems, enabling modular robots to perform more advanced tasks with greater efficiency and accuracy.

A robotic system can be characterized as manually configurable or self-reconfigurable based on the extent of autonomy of the connecting mechanism [65]. Magnetic docking systems are commonly used in manually configurable systems, whereas electromechanical docking systems are utilized in self-reconfigurable systems. In all of these systems, tradeoffs exist between size, strength, speed, power, and complexity, as defined below. Table 2.1 provides an overview of the connection characteristics of self-configuring modular robots.

(i) Size - To minimize the impact on payload capacity, the mechanism should

be designed to be as compact as possible. A smaller mechanism also allows for multiple attachment points on the robot's body, increasing flexibility and versatility.

(ii) Strength - It is crucial for the system to have sufficient strength to withstand any potential impact or motion that may occur during its intended use, ensuring that the overall configuration remains intact at all times. The mechanical strength of a configuration is determined by its weakest link, which is typically the strength between two modules in the configuration

(iii) Power - Connection and disconnection have to be as efficient as possible since the power available in a module is limited.

(iv) Complexity and Cost - The mechanism should be simple enough to manufacture and assemble without requiring a high degree of technical expertise, while still being cost-effective and reliable.

2.1.1 Passive

Based on actuation, attachment mechanisms can be either active or passive. An active mechanism consists of hardware components such as hooks or latches which would require an actuator to establish a connection. By contrast, a passive mechanism lacks actuators and is generally equipped with intelligent mechanical design features which form connections. Yi [75] has developed Puzzlebots (Fig. 2.1) which can physically couple with each other with no energy consumption while maintaining individual mobility. The body of the robot measures 50 mm in width, 50 mm in depth, and 35 mm in height, and is 3D printed with thermoplastic polyurethane (TPU). Each robot has knobs and holes equally

distributed along the length of the body so that robots can couple by inserting knobs into holes as seen in Fig. 2.1(a). When robots approach a gap, the initial robot to depart from the platform will experience gravitational force and become inclined, leading to the arrangement depicted in Fig. 2.1(b). The connection is uncoupled when the modules are on a flat surface. The robotic system can form long chain-like structures and cross gaps up to half the size of the whole assembly.

This coupling mechanism offers several benefits, including energy efficiency. As the coupling process does not require any additional energy apart from what is needed for the robot's movement, it helps conserve energy and improves the robot's overall efficiency. However, there are also some significant drawbacks to this mechanism that must be considered. One of the most significant drawbacks is the high degree of precision required for the locking mechanism to engage, which becomes even more challenging at a smaller scale, potentially limiting its use in certain applications. Additionally, this mechanism has no force transfer between modules on a flat surface, which can limit the types of tasks the robot can perform. The range of motions and orientations between modules is also limited due to the mechanical elements that must engage for the coupling to occur, which can restrict the robot's flexibility and adaptability in certain scenarios.

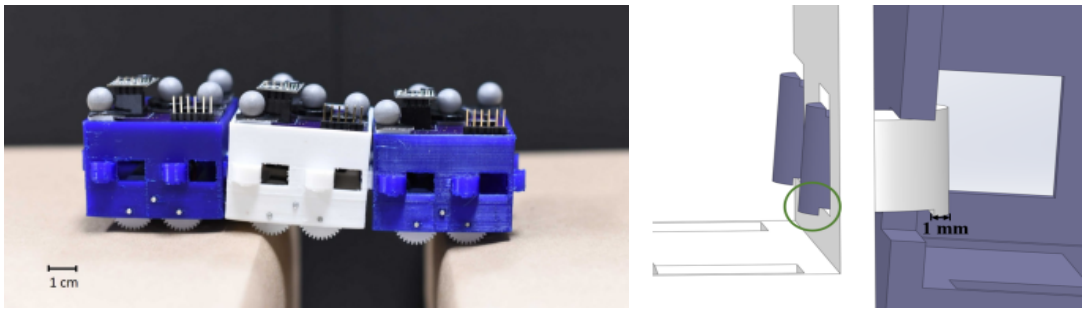

(a) (b)

Figure 2.1: Puzzlebots (a) Three robots collaborate to cross a gap between two platforms. (b) A successful coupling example with a hook of width 1mm. When the robot is tilted due to gravity. The hooks are able to block the movement of the robot's body.

2.1.2 Electrostatic

Electrostatic coupling is gaining popularity in mm- and cm-scale robotic systems due to its low power consumption, miniaturization capability, and flexibility in design. It is an energy-efficient mechanism that is practical for low-power systems and can be easily integrated into small robotic systems.

Karagozler et al., [35] has developed a robust latching principle employing electrostatic adhesion, which can generate an adhesion force of up to $0.6N/m^2$. The paper describes a mechanism that uses electric fields to generate frictional shear forces between flexible, capacitively coupled electrodes. The system avoids the negative effects of peeling by using shear forces instead of direct electric field attraction. The mechanism consists of two genderless "faces" made of a star-shaped plastic frame to which multiple electrodes are attached (Fig. 2.2(a)). Each electrode is made of a thin aluminum foil coated with dielectric film wrapped and glued onto a plastic panel. The faces have normal surfaces that create the shear forces necessary for the mechanism to function. According to Karagozler et al., although not yet efficient, this type of docking system is

capable of transferring power between linked modules and enabling communication between them. Electrostatic adhesion has also been deployed in insect scale microrobots to achieve inverted and vertical climbing of HAMR [10], and perching and takeoff of RoboBee [16].

Although electrostatic coupling provides a strong latching force, it can be effortlessly disengaged when the applied force is perpendicular to the electrode surface rather than parallel. Environmental factors such as dust can be challenging to deal with at smaller scales because of the exponential relationship between capacitance and inter-electrode distance. Even a minor increase in the separation between the electrodes can significantly decrease the generated force, causing them to detach with a relatively small force.

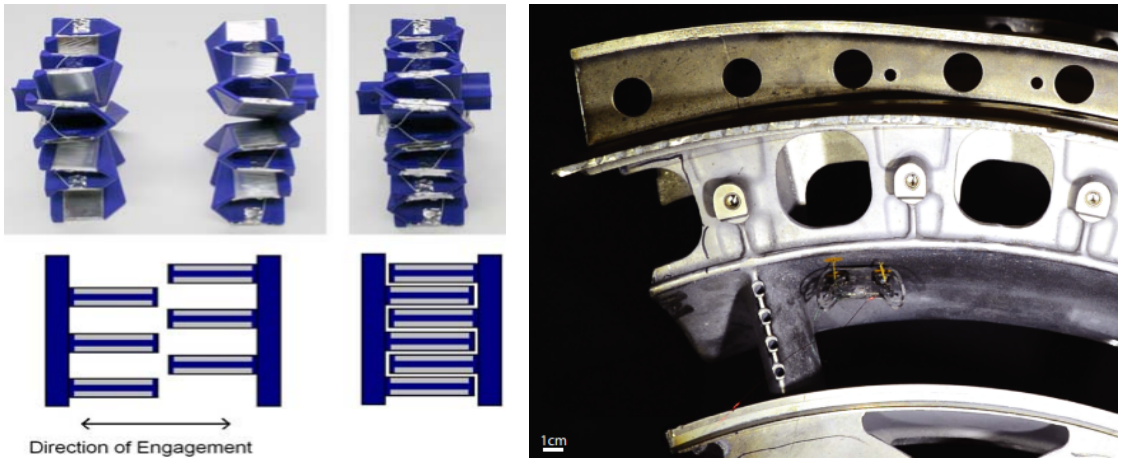

(a) The two faces of the latch engaging (b) HAMR-E

Figure 2.2: Electrostatic attachment in different robot systems. (a)Electrostatic latching developed by Karagozler et al. [35] (b) Inverted locomotion on the inner surface of a commercial jet engine[10].

2.1.3 Magnetic

Magnetic coupling is a popular choice in modular robots due to its high holding force, simple mechanism, non-contact operation, no power consumption during coupling, and flexibility in design. It is suitable for heavy-duty applications and low-power systems, and the non-contact operation reduces wear and tear on the system. For example, each module of M-TRAN I and M-TRAN II systems [40] employs four magnetic connectors arranged in a square pattern, allowing the modules to dock together in any orientation. When two modules approach each other, the magnetic connectors align and attract each other, pulling the modules together until they are in contact. To disengage, a small amount of force is applied to one module, using shape memory alloy (SMA) coils and a nonlinear spring, to break the magnetic connection, after which the modules can be separated.

Another popular example is the M-Blocks system [59] developed at MIT, its unique design allows modules to form magnetic hinges on any of the twelve edges of the cubes using the twenty-four diametrically polarized cylindrical magnets. To solve the alignment problem, eight disc magnets are embedded in each of the six faces, arranged in an eight-way symmetric pattern to maintain gender neutrality. These alignment magnets pull a module into alignment but do not add significant holding force to the face bonds. The design ensures that the strength of a hinge bond is not dwarfed by the strength of the face bond when the modules are flush and well-aligned.

Magnetic couplers can provide high holding forces between modules. Generally, a higher bond strength does not hurt and keeps the system from falling apart under static and dynamic loads, but detaching would be an energy-

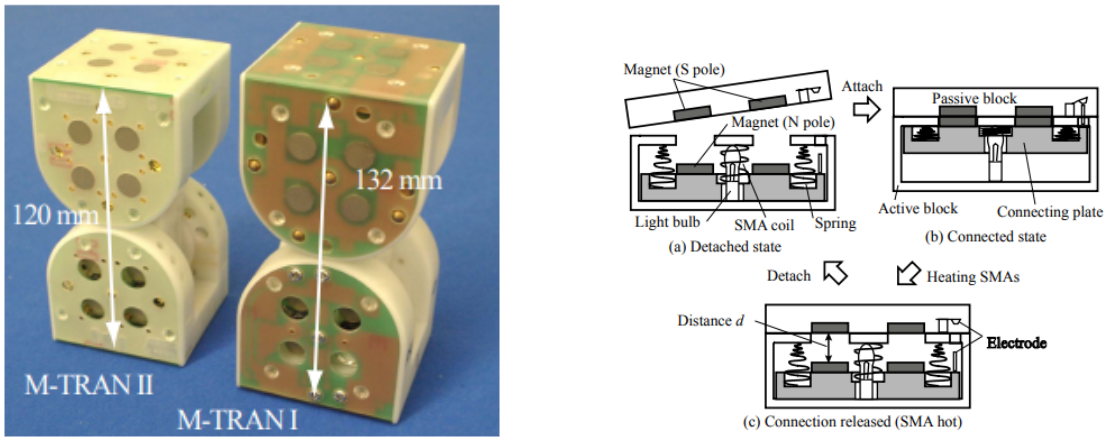

(a) (b)

Figure 2.3: (a) M-TRAN I and M-TRAN II modules (b) Magnetic docking mechanism in M-TRAN II. [40]

Name	Size	Strength	Power
M-TRAN II [40]	60 mm	85 N	4W
M Block [59]	50 mm	23N	0.6W

Table 2.2: Features of magnetic docking mechanisms

intensive task. At the centimeter scale, ambulatory robots typically have low inertial mass. Magnetic couplers generate strong forces as the distance between them decreases, which can cause the modules to rapidly pull together, potentially leading to high impulse forces that could damage the microrobots. Therefore, magnetic coupling is not a suitable option for centimeter-scale robots.

2.1.4 Electromechanical

Electromechanical coupling mechanisms are popular in current modular robots for several reasons. They are reliable and provide a consistent connection between modules. They also offer a high degree of flexibility in terms of module configurations and can be easily customized to fit different applications. Addi-

tionally, they require relatively low power and can be implemented in low-cost, low-weight designs. Finally, they are not affected by environmental factors such as dust or temperature, which can be a challenge for magnetic coupling mechanisms.

The modules in Poly-Bot G2 employ pins and holes fastening for forming a connection [76]. The docking interface consists of an SMA wire-actuated retraction spring mechanism for severing the connection. An essential characteristic of such coupling mechanisms is that it only consumes energy during the connection and disengagement processes, but none when attached. Another example of SMA actuated disconnection mechanism is found in an Alligator-inspired modular robotic system [31]. Here, two locking blocks are used for connecting a head and tail of a module to the larger robot frame.

Although permanent magnets were used for connection in the former series of M-TRAN, the docking systems in M-TRAN III modules feature motors and hooks to form a latch connection [41]. It is faster and stronger in connection and consumes less power than the former prototypes. Some alignment error (5 mm) between two surfaces is allowed for in the connection by a proper design of the hook and the cavity on the female surface.

One of the main drawbacks of electromechanical coupling for cm scale robots is, as the size of the robots decreases, the amount of power available for the robot's operation decreases, making power consumption a critical concern. Electromechanical coupling requires the use of motors or other actuators to drive the coupling mechanism, which can consume a significant amount of power. This can limit the robot's range, endurance, and overall performance. Additionally, electromechanical coupling mechanisms can be complex and dif-

ficult to miniaturize, making them unsuitable for small-scale robots.

2.1.5 Electromagnetic

Electromagnetic coupling in modular robots involves the use of magnetic fields to connect and disconnect modules. One example of this is the Molecule robot, developed by Kotay et. al., [39] in which modules contain an electromagnet that can be switched on and off to connect and disconnect from neighboring modules. This allows for flexible configuration and reconfiguration of the robot.

Electromagnetic coupling offers an advantage over magnetic coupling as it allows connections between any two docking units without needing to flip the docking surface, and there is no additional mechanism required to undock or repel a linked module. However, electromagnetic connectors can be less energy-efficient because electrical power is required to establish and sustain the magnetic field. The use of magnetic fields in electromagnetic coupling may also interfere with the operation of other sensitive components of the robot, such as sensors or communication systems.

In summary, the evaluation of different attachments for a cm-scale ambulatory microrobot shows that electromechanical attachment works best for the coupling mechanism. Passive mechanisms, which do not require additional energy for coupling, have benefits such as energy efficiency but drawbacks such as the need for high precision and limited force transfer. Electrostatic coupling, which uses low power consumption and flexibility in design, has challenges with disengagement and environmental factors. Magnetic coupling, which has high holding force, and non-contact operation, is suitable for heavy-duty ap-

plications but can potentially lead to high impulse forces that could damage the microrobots. Overall, electromechanical attachment provides a balance between energy efficiency, precision, force transfer, and flexibility, making it the optimal choice for the coupling mechanism in a cm-scale ambulatory microrobot.

2.2 Actuator strategies for microrobots

Actuation strategies are of utmost importance for microrobots, as they are responsible for providing the necessary force and deflection required for locomotion. In addition, they must achieve high power densities to enable autonomous locomotion despite the limited payload capacity of onboard power supplies. Choosing the right microactuator for a specific application is a crucial task that requires careful consideration of several characteristics. These include the size of the actuator, its range of motion, speed, precision, resolution, power consumption, durability, and cost-effectiveness. The size of the actuator must match the scale of the application, while the range of motion and speed must meet the requirements of the task at hand. Precision and resolution are also important considerations, particularly for applications that require high accuracy. Power consumption and durability are also critical factors to consider, as well as cost-effectiveness to ensure the feasibility of the overall system. Therefore, a correct choice of actuation for a particular application needs careful consideration of the various characteristics of the available microactuators. The following section will discuss the different actuators that are prevalent in microrobot research.

Actuators used in conventional scale robots cannot be directly applied to

Type	Limits	Force	Response time	Power density
SMA	Thermal response	L^2	L^2	L^{-2}
piezoelectric	Resonance	L^2	L^1	L^{-1}
Lorentz-force	$J \propto L^{-1}$	L^2	L^1	L^{-1}
Electrostatic	Breakdown voltage	C	L^2	L^{-4}

Table 2.3: Scaling laws for different actuators [55]

cm-scale robots due to several reasons. One reason is that the physical laws governing the behavior of materials change at the microscale, which affects the performance of conventional actuators when scaled down. As the scale of the system decreases the effect of surface forces, which scale as L^2, begin to dominate Newtonian forces, which scale with mass (L^3). Additionally, as the size of the robot decreases the components become more sensitive to noise, have higher energy density requirements, and are more challenging to fabricate with the required precision. This leads to the need for new and specialized actuators, such as piezoelectric, shape-memory alloy, and electrostatic actuators. Table 2.4 gives an insight into the important parameters, characteristics, and features of the most common microactuators.

Type	Displacement	Time response	Force/Torque
EM micro motor	Rotating	100Hz	1mNm
EM thrust type	Length of Solenoid	50Hz	10mN
Electrostatic micro motor	Rotating	1kHz	10pNm
Bimorph piezoelectric	1-5% of length	1kHz	10N
Wired SMA	3% of length	5Hz	10kN/cm
Polymer	1-50% of volume	1Hz-10Hz	1N

Table 2.4: Characteristics of micro actuators

2.2.1 Piezoelectric

The most prevalent choice for actuation in microrobots is piezoelectric actuators. Due to the fast response (order of kHz), high resolution (nm), and high moving speed. The drawbacks are the high input voltages and small strokes, which call for additional mechanisms to amplify the stroke. The most common technique to increase the stroke is multi-layer actuators and adding passive elements to convert the longitudinal strain to bending movement. Such actuators include unimorphs and bimorphs [11]. Another common technique to increase the stroke of piezoelectric actuators is leveraging additional passive elements. Few such approaches include transmission mechanisms such as the 5 bar spherical linkage in HAMR, exploitation of buckling [67, 50] and nesting actuators [69]. Bio-inspired robots developed using Piezoelectric actuators are inchworm robot [27], three-legged robot [47, 26], HAMR[4], myriapod robot[22], RoboBee [74] and fish robot [52].

2.2.2 Shape Memory Alloy (SMA)

Shape memory alloys are materials that retain their shape and can recover to it with the change in temperature. SMA actuators are unidirectional linear actuators, (i.e.) they can generate force only in a single direction, and thus require some restoring force for repetitive operation. Hence, a single DOF requires an antagonist pair of SMA actuators.

SMA is a popular choice for actuation for microrobots largely due to their ease of powering, control, and high power density. SMA materials are actuated simply by Joule heating and hence require an on-off current source (i.e., square

waveforms). Hoover et al., developed a hexapod robot RoACH[25], Menciassi et al., developed a robotic crawler inspired by earthworms [48], Koh et al., developed Omegabot with a novel gait which mimics an inchworm [38], and Wang et al., proposed a micro-robot fish propelled by a biomimetic fin which can achieve a max speed of 11 cm/s [71].

2.2.3 Polymer actuators

A polymer actuator possesses several characteristics that make it a desirable choice for certain applications. In general, these materials are pliable, lightweight, less prone to fracture, and generally inexpensive. Polymeric microactuators can produce larger displacements compared to those generated by SMA-based actuators, and in some cases, the response can be faster. A common choice of material is IPMC (Ionic Polymer Metal Composite) due to its ability to produce large bending displacement in comparison to piezo actuators. Several actuators have been realized using IPMC actuators such as swimming microrobot [17], micropump [18], and micro gripper [46]. IPMC has gained attention due to its softness, lightness, and relatively low driving voltage. The earliest IPMC actuator developed for a legged robot was by Tadokoro et al., [66] called Elliptic Friction Drive (EFD actuator element). In 2003, Kim et al., developed a ciliary-based 8- legged microrobot [36]. However, it also has a number of drawbacks, including high driving currents, poor repeatability, and limited durability in dry environments.

2.2.4 Electromagnetic actuators

Electromagnetic actuators have been a dominant choice of actuation for day-to-day conventional machines primarily due to their high efficiency in converting electrical energy to mechanical energy. They offer several advantages such as simple control, low cost, and fast response. Another advantage of using electromagnetic actuators is that they have very low voltage requirements. The voltage used to drive them can range from 0 to 24V. However, electromagnetic actuators are not favored at the millimeter scale because of the difficulty in fabrication, unfavorable scaling effects, and the high Joule loss due to the high resistance of a micron-diameter wire.

Rotary EM actuator with a diameter of 4.6 mm has been developed in the late 90s by Hisanaga and Teshigawara [21]. In rotary motion, the sliding and rolling of components lead to significant frictional losses, which can result in decreased efficiency and increased wear and tear of the components. Reciprocating motion, on the other hand, involves less sliding and rolling, making it more efficient and suitable for microrobotics. The linear electromagnetic actuators are used for inchworm robots [28, 45, 62, 42]. Electromagnetic actuation is also regarded as a successful driven strategy for micro flapping wing robots [58, 77, 5, 6], although it may result in more energy cost and heat production.

Advantages of linear electromagnetic actuation in bioinspired robots include high force capabilities, precise control, and flexibility in motion. The ability to generate strong and reversible forces without physical contact with the environment allows for efficient and smooth locomotion. Additionally, the simplicity of design without the need for complex mechanical linkages makes the robots lightweight and potentially more reliable. However, there are also disadvan-

tages, including the reliance on a power source for generating magnetic fields, which may impact runtime and energy efficiency. The potential for heat generation during operation and electromagnetic interference with other electronic devices in the robot or its environment may also pose challenges.

In summary, piezoelectric actuators are popular due to their fast response, high resolution, and high moving speed, but require high input voltages and additional mechanisms to amplify stroke which in turn increase the power consumption and size of the mechanism, both of which are limited in a microrobot. SMA actuators are easy to power and control but is difficult to achieve high speeds of operation because these are limited by the cooling times. Also, another limitation is that the maximum attainable contractions of SMA wires do not exceed 5%. Polymer actuators, such as IPMC, are pliable and lightweight but have drawbacks including high driving currents and limited durability. Electromagnetic actuators offer simple control, low cost, and fast response, but may have fabrication challenges at the millimeter scale and high Joule loss. Linear electromagnetic actuators have advantages in bioinspired robots, including high force capabilities and precise control, but also rely on a power source for generating magnetic fields. Overall, an electromagnetic actuator is suitable for the current mechanism due to its low operating voltage, precise control, and flexibility in motion.

CHAPTER 3

ACTUATOR AND SPRING DESIGN

The previous chapter established that electromechanical docking and electromagnetic actuation are suitable for the docking mechanism in cm-scale ambulatory microrobots. This current chapter focuses on the actuator and spring design, which are essential components of the docking mechanism. The chapter explores the initial designs proposed, including one that uses flexure elements to form a connection similar to snap-fit assembly, but it was discarded due to the use of SMA. Another design inspired by a rail car coupler was also explored but was discarded due to the high precision required, which is impractical at the given scale of operation. This chapter aims to present a new and improved design for the actuator and spring, discussing the various design considerations.

3.1 Initial design

The first design aimed to minimize power consumption by only using active actuation during undocking. It consisted of a curved flexure element and a stopper to create a docking mechanism, as shown in Fig.3.1(a). The flexure element allowed for passive docking, where no additional actuation was necessary to connect the modules while it does require actuation to detach. During docking, the stopper pushed against the curved elements, causing them to bend in the vertical direction as illustrated in Fig.3.1(b). The two curved parts would swing inwards during the docking process and then return to a neutral position once docking was complete. After docking, the curved elements were mechanically locked in place through interference, as seen in Fig.3.1(c).

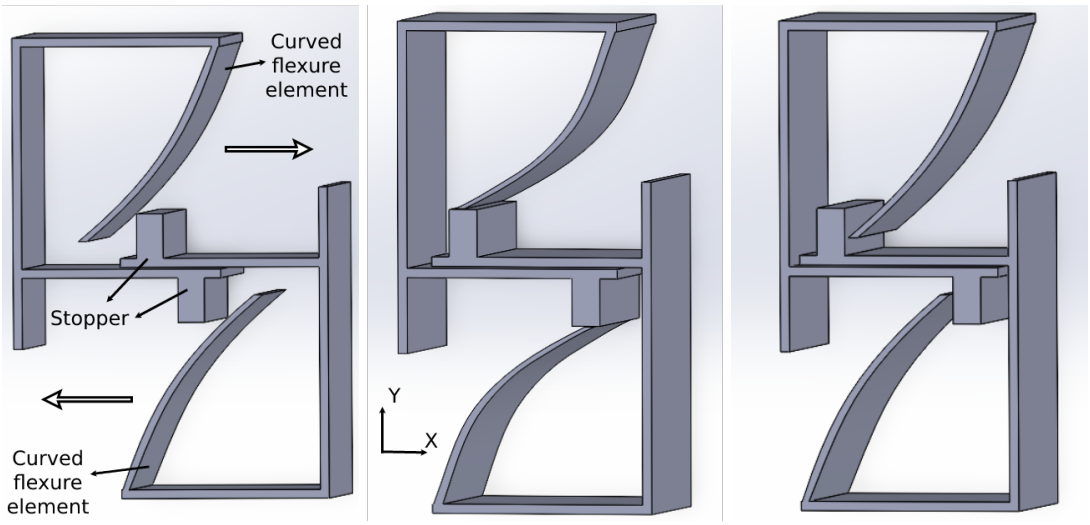

Figure 3.1: (a) The two parts of the docking mechanism approach each other to form a connection. The arrows show the direction of motion. (b) The stoppers push the curved flexure elements after coming into contact. (c) The stopper moves past the curved element resulting in mechanical interference. This is the final orientation once docking has been achieved.

To unlock the mechanism, an actuator is required to bend the curved elements in the Y direction. Due to the high force required for deforming the curved elements, Shape Memory Alloy (SMA) was considered a viable option. SMA could provide the necessary force, but it has a slow response time and requires large currents to drive, which in turn increases power consumption.

Furthermore, to allow for the bending of the flexure element during actuation this design had slack in the X direction along the length as well as Y direction, which could result in reduced stability and alignment. Additionally, any off-axis twisting (greater than 10^{circ}) could result in the detachment, posing a potential issue in reliability.

The second design draws inspiration from the Janey coupler[1], a semi-automatic coupling system commonly used in modern rail cars and locomo-

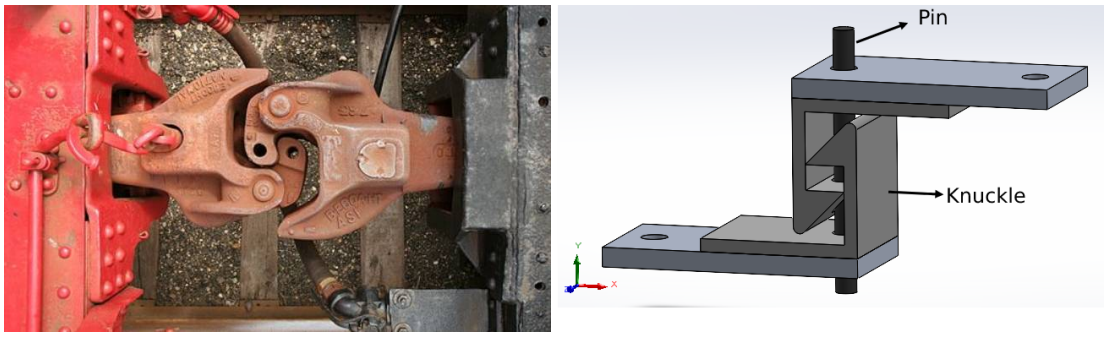

(a) (b)

Figure 3.2: (a) Mated Janey coupler in rail cars as seen from above. (b) Coupling mechanism inspired by Janey coupler

tives. The Janey coupler consists of two interlocking knuckles and a pin that holds them in place once a connection is formed. Upon impact between rail cars, the open knuckles swing into the closed position, and a lock drops into place to secure the connection, although some slack may remain between the knuckles. In our design, we aim to replicate this concept, but instead of relying on gravity for the pin to drop into place, we require a linear actuator to lock the connection. However, a major challenge in the design is achieving the high precision required at a smaller scale for inserting the pin into the hole. Fig. 3.2(b) depicts the design inspired by the Janey coupler, with the need for a linear actuator to ensure precise and reliable locking of the connection.

3.2 Final design

The final design features a pin lock fastening, with an actuated pin that can be inserted and removed from a passive locking component(see Fig. 3.3). To conserve power in the unactuated state, we limit the actuation of the pin to locking and unlocking only. This is in contrast to electromagnetic docking mechanisms

which typically employ continuous actuation. To ensure that the pin remains in place when not being actuated, we have inserted it through a planar spring that allows it to return to its neutral position after actuation or in the presence of external impacts. In its unactuated state (as shown in Figure 3.3), one end of the pin is partially inside the coil while the other end passes through a locking structure. This design ensures that the pin stays in position under loading along the x-direction and restricts any out of plane rotation of the pin.

After careful consideration of various actuation strategies, electromagnetic actuation was determined to be the optimal choice for this design. Electromagnetic actuators utilizing a permanent magnet scale similar to piezoelectric actuators (refer to Table 2.3). The decision was based on their compact size and simple drive electronics. Unlike some other actuation methods, electromagnetic actuators do not have inherent limitations on the range of motion, as they depend on the strength of the magnet and the length of the coil, providing us with the flexibility to generate the desired displacement. The required displacement for our application is 1 mm, as the counterpart is a carbon laminar sheet with a thickness of 50 μm and a hole larger than the pin to fit. To minimize magnet displacement, we utilize low-displacement actuators. This approach guarantees that the coil experiences larger average magnetic fields while maintaining low currents, leading to a significant reduction in both the current and power requirements. Consequently, this simplifies the power electronics involved in the system.

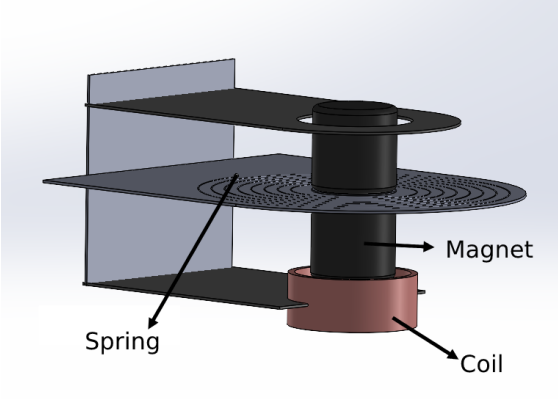

Figure 3.3: Final design of the mechanism. The spring is in its neutral state and the mechanism is not actuated.

3.3 Electromagnetic actuator design

The EM actuator is comprised of a permanent magnet and coil placed coaxially. A Neodymium grade N52 magnet (D11-N52, K&J Magnetics, 1.6mm diameter, and height) is used to create the magnetic field. To minimize the current consumption, we selected the N52 grade magnet, which is known to be the strongest grade magnet available. This size was chosen because it generates the desired displacement while consuming less current compared to weaker magnets. Despite its strength, it is also one of the smallest magnets available in the millimeter size range, making it an ideal choice for our compact design. Copper is chosen as the coil material due to its low resistivity. The coil is hand wound from 50μm-thick Copper wire with $n_{turns} = 4 \times 50$ number of times. We give the coil a radial clearance of 200µm (coil inner radius = 0.8mm + 0.2mm = 1mm) to avoid any collisions with the magnet during motion. The coil has a height of 3 mm, with a resistance of approximately 17Ω. The force experienced by the coil is given by

$$F_{Lorentz} = B_{radial}(x) * I_{coil} * l_{coil} \tag{3.1}$$

where $B_{radial}(x)$ is the magnetic field seen by the coil at a separation of x from the center of the magnet. The coil is driven by a square wave using a motor driver and microcontroller.

3.4 Spring

In our mechanism, the spring is essential to provide the necessary restoring force to maintain the pin (magnet) position in the absence of Lorentz force. In regard to the current application, the spring should (1) have a predictable and constant spring rate, (2) be easily manufacturable, and (3) be compact in size.

The spring rate is the ratio of the force exerted by the spring to the displacement caused by it. A predictable spring rate means that the spring behaves consistently and reliably under different loads and displacements, allowing for accurate and repeatable actuator performance regardless of changes in operating conditions. Furthermore, a constant spring rate, where the spring rate remains relatively unchanged with displacement, simplifies the control of the actuator, as the displacement versus current relationship can be linearly correlated, making it easier to achieve the desired displacement and motion characteristics.

In addition, the spring should be easy to produce and assemble with the rest of the components of the actuator. The manufacturing process should be cost-effective, scalable, and repeatable. The spring should also have a long service life and low maintenance requirements.

In addition to a predictable and constant spring rate, the size and weight of the spring are important considerations in the design of the actuator. The

given mechanism being an addition to a microrobot, it is essential to keep the footprint of the spring compact to minimize its impact on the dynamics of the microrobot. Moreover, the compact size and lightweight design of the spring contribute to the overall weight reduction of the actuator, which is critical in microrobotic applications where size and weight are limited.

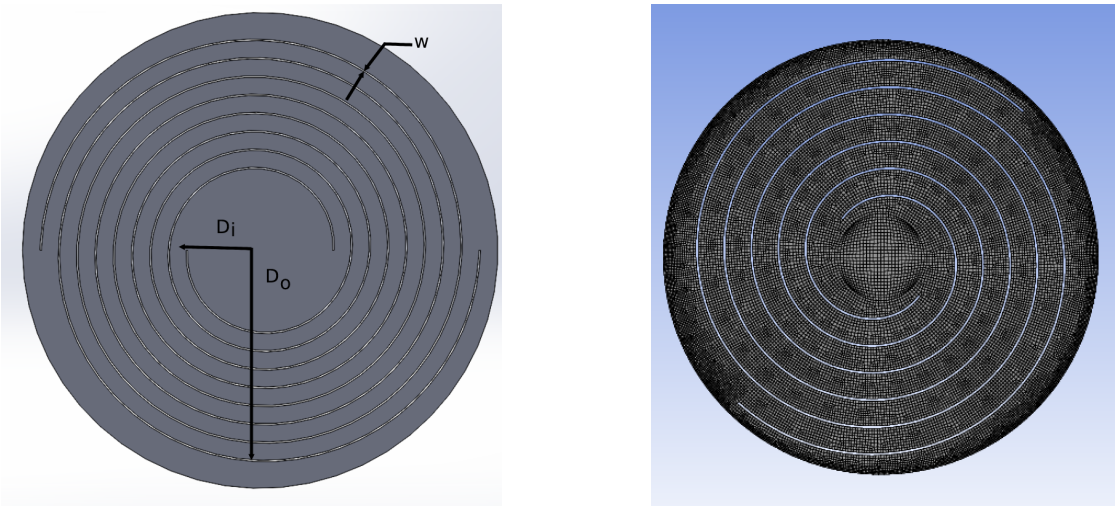

(a) Planar spiral spring (b) Finite element mesh

Figure 3.4: Planar spring design

The coils of the spring are formed by extracting two spirals of material from a circular flat sheet of steel. Laser cutting was used to remove spirals in the shape of involutes from this design. The shape of the cut out spiral is that of an involute of a circle. The result of using two involute shaped cuts, 180^0 apart, is that the coils are also involutes having constant width as they progress out from the center. The material cuts in planar spiral springs do not necessarily need to be in the shape of involutes. Cuts of various spiral shapes would result in planar spiral springs but of different geometries. Springs of several coils can be made by the introduction of nonintersecting material cuts. Two cuts, resulting in two coils, is the minimum, where a coil is defined as the arm or spline of material that connects the outer ring to the center. An advantage of planar spiral springs

is that they are potentially inexpensive to make in large numbers using any number of fabrication methods, including stamping, laser cutting, and water jet cutting out of sheet steel as opposed to the wire winding process used to make typical springs. Also, as conical springs have increased lateral stability compared to cylindrical helical springs [34], planar spiral springs may be quite stable too.

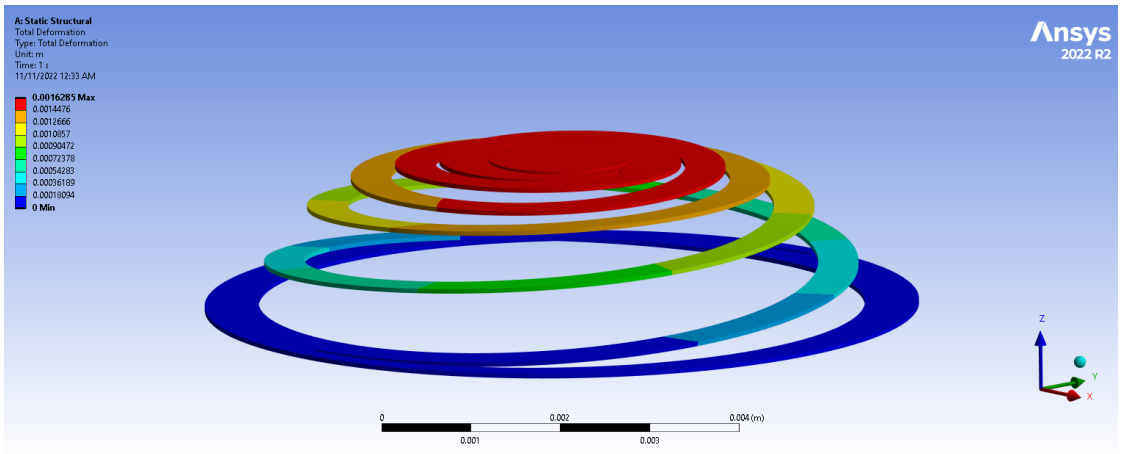

Figure 3.5: Visualization of spring deflection. The color map represents the displacement from the neutral state, where blue indicates minimal deflection while red indicates maximal deflection. The maximum deflection observed is 1.6mm.

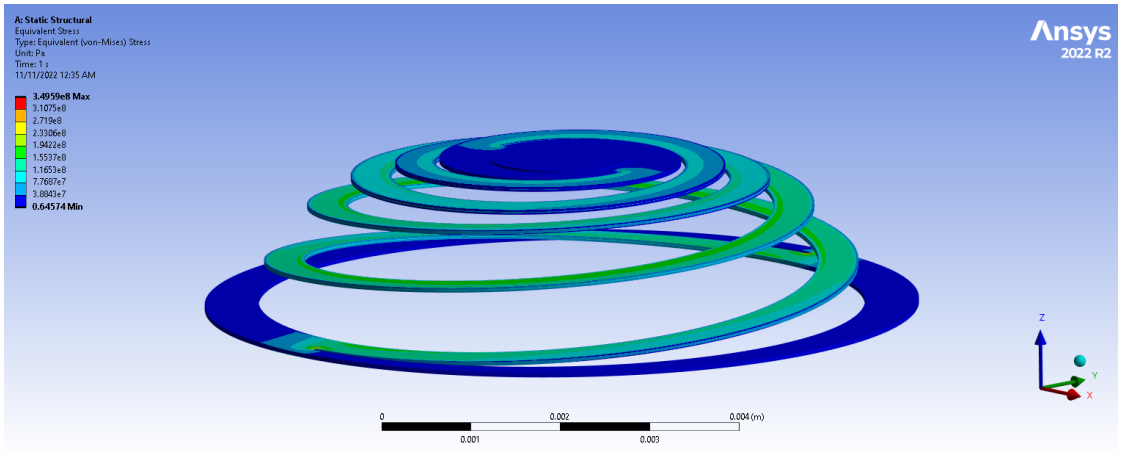

Figure 3.6: Von mises stresses in spring

Due to the lack of a straightforward design theory for planar spiral springs, we chose to perform a Finite element analysis to determine the pitch of the spi-

ral, and the number of turns. An alternative choice to FEA is a rigorous and thorough set of experiments on a statistically significant number of planar spiral springs. Such a test program, however, would be time consuming and expensive. The FEA analysis was performed in ANSYS. The parameters of the spring design searched were the pitch of the spiral (i.e. the rate of change of radius), and the number of revolutions. The thickness of the material and cut width were 50 μm and 20 μm respectively and remained constant during the parameter search. The diameter of the central platform was set to 2 mm so as to accommodate a magnet of diameter 1.6 mm. Fig. 3.4(b) shows the finite element mesh for the model of a spring. Fig 3.7 shows the force-deflection curve of the modeled spiral planar spring. The spring constant determined from FEA is 6.5 mN/mm. The spring parameters are shown in Table 3.1

Y	190 GPa	t	25 μ m
Pitch	0.5mm %	w	20 μ m
k	6.5mN/mm	N	4
Inner Dia D_i	2 mm	Outer Dia D_o	6mm

Table 3.1: Spring parameters

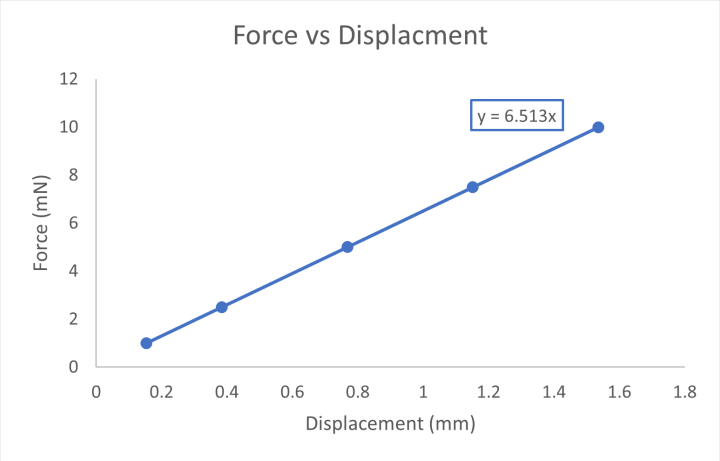

Figure 3.7: Force-Deflection curve of planar spiral spring from FEA

CHAPTER 4

POWER AND CONTROL ELECTRONICS

For the current prototype, we have implemented external power and driver electronics. Current for the coil was supplied by L293D integrated circuit (IC) motor driver. We used an Arduino Uno microcontroller to supply the logic inputs to the IC.

The L293D is a popular integrated circuit (IC) commonly used as a motor driver, specifically for controlling DC motors or stepper motors. It is a dual-channel H-Bridge IC capable of controlling up to four DC motors or two stepper motors, making it suitable for various robotics and automation applications. The L293D is designed to provide bidirectional drive currents of up to 600 mA at voltages from 4.5 V to 36 V. The primary reason for choosing an H-bridge is the ease of miniaturization and the readily available options at the millimeter scale such as the DRV8837 and PAM8016.

4.1 Control signals

In the experiments performed, we used DC square waves as control signals which were generated using an Arduino Uno microcontroller board. The PWM pin on the board was utilized to alter the voltage signal, which allowed us to vary the amplitude of the signal. This, in turn, controlled the displacement of the actuator. In addition, the logic pins on the board were employed to control the direction of actuation. This enabled us to control the movement of the magnet in different directions. The pulse width of the control signals used in the

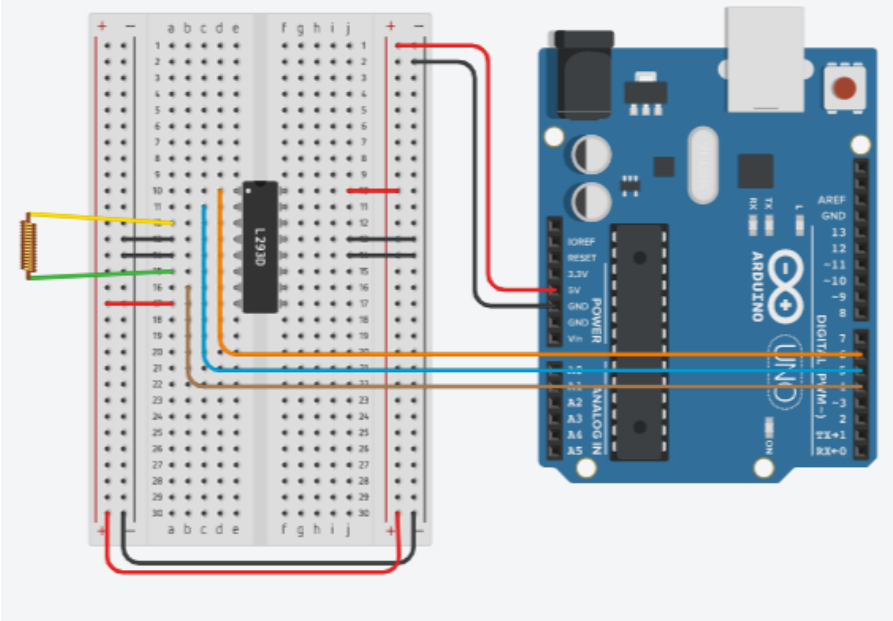

Figure 4.1: Schematic of the electric circuit

docking experiments was on the order of seconds.

Overall, the use of DC square waves generated using an Arduino Uno and the utilization of the PWM and logic pins on the board proved to be an effective method of controlling the pin in the docking mechanism. This approach allowed us to accurately and precisely control the movement of the pin/magnet in various directions.

4.2 H-Bridge

The H-bridge is a typical DC motor control circuit, named after its resemblance to the letter H. The H-bridge is shown in detail in Fig. . An H-bridge is an electronic circuit that reverses the voltage/current at both ends of the load or output to which it is connected. Robots and other practical applications use

these circuits for DC motor direction, speed control, DC-AC converters, a few types of DC-DC converters, and several electrical equipment. Table 4.1 shows the operation of the H-bridge for different states of the gates (S1-S4).

4.2.1 Working principle

An H-bridge is built with four switches. A positive voltage is provided across the motor when switches S1 and S4 are closed and S2 and S3 are open. This voltage is switched around by opening the S1 and S4 switches and shutting the S2 and S3 switches, enabling the motor to run in the other direction. Typically, bi-polar or FET transistors or, in some high-voltage applications, IGBTs serve as the switching components. Switches S1 and S2 (or S3 and S4) should never be closed simultaneously in a bridge since doing so would result in an extremely low resistance, in effect short-circuiting the power supply. This issue is known as a shoot-through.

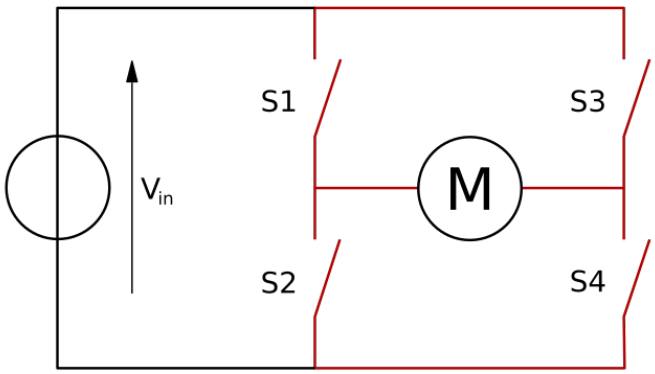

Figure 4.2: H-bridge circuit

4.2.2 Drive modes

The H-bridge configuration is typically used to switch the polarity or direction of the motor, but it may also be used to 'brake' the motor, bringing it to an abrupt halt by shorting its terminals. When a circuit is shorted, the kinetic energy of a rotating motor is quickly converted into electrical current. The alternative is to let the motor "free run" until it stops as it is essentially cut off from the circuit.

S1	S2	S3	S4	Result
1	0	0	1	Magnet moves up
0	1	1	0	Magnet move down
0 1	1 0	0 1	1 0	Magnet returns to neutral state

Table 4.1: Drive modes of an H-bridge for the mechanism. The "on" state of the switch is represented by "1", while the "off" state is represented by "0."

In conclusion, the successful implementation of power and electronics using an H-bridge motor driver IC and Arduino microcontroller on a conventional scale is a significant achievement. As the project progresses, future work can focus on miniaturizing the motor driver by utilizing off-the-shelf H-bridge drivers. Additionally, for a completely autonomous ambulatory microrobot, the onboard microcontroller can be utilized to generate the control signals, further enhancing its capabilities.

CHAPTER 5

RESULTS

We conducted a series of experiments to verify the stiffness of the spring, evaluate the holding force of the coupling mechanism, and measure the current consumption of the actuator. Firstly, we performed a spring validation experiment to ensure that the spring's stiffness falls within the error margin of the estimated value. This is crucial for the actuator to generate the desired displacement for a given current. Next, we tested the actuator to obtain a current versus displacement graph to ensure that the actuator is consuming current within our design criteria. Lastly, we conducted a loading test to determine the maximum holding force of the coupling mechanism. These experiments were performed to ensure the robustness and accuracy of our system.

5.1 Spring Validation

We conducted an experiment to verify the stiffness constant of the fabricated spring. The spring was loaded with weights, as shown in Figure 5.1(a) while being firmly grounded to ensure a vertical loading. Magnets of known mass were attached to the central platform to apply a constant force. The deflection of the spring was measured by capturing images using a Nikon DLSR camera and analyzing them using Python code (provided in the appendix). The deflection of the spring from its neutral state was calculated using the images, with a reference image with a known scale used to obtain the mm/pixel calibration value. The correlation between the deflection of the spring and the applied torque was plotted, as shown in Figure 5.2, and a linear fit was used to determine the slope of the plot, which represents the spring constant.

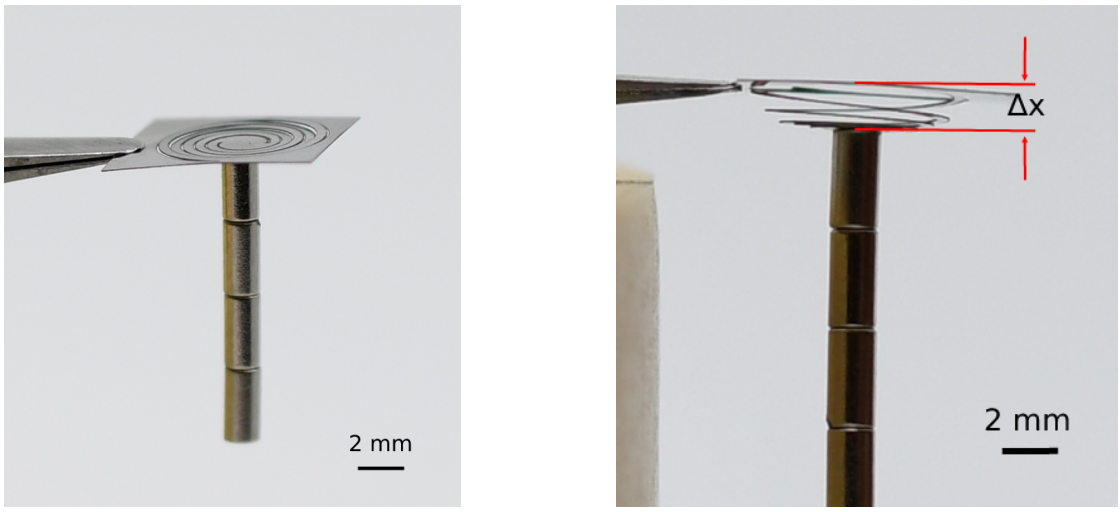

(a) (b)

Figure 5.1: (a) Magnets stacked together for loading the spiral spring (b)Deflection measurement to determine the spring constant of the planar spiral spring.

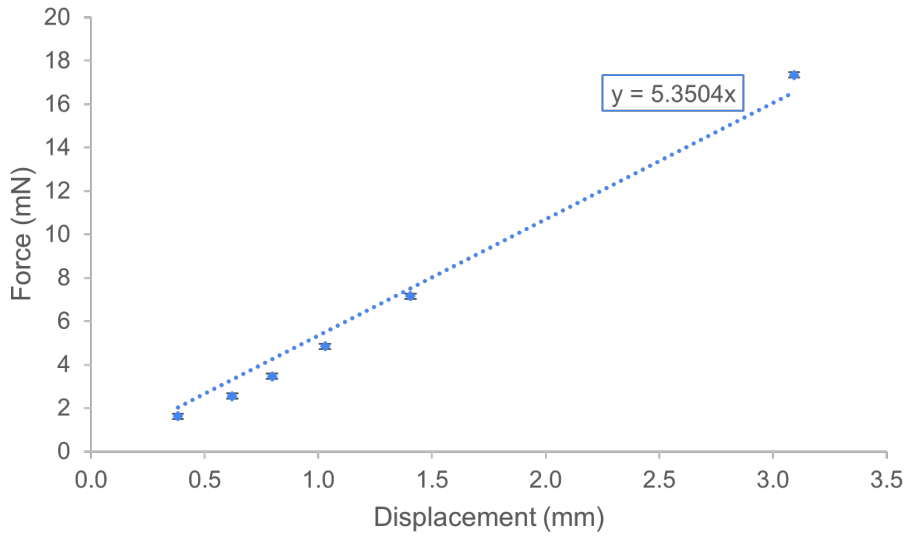

Figure 5.2: Spiral spring characteristic graph depicting the linear nature of the spring.

Finite element analysis was used to determine the stiffness of the designed spring, which was found to be 6.5mN/mm. However, the estimated stiffness of the spring manufactured was 5.35mN/mm, resulting in a 20% error in the

stiffness value. The significant difference between the theoretical and actual stiffness of the spring could be attributed to several factors. Firstly, the laser cutting process generated high thermal temperatures, causing high thermal strains in the thin steel (50μm) used for the spring, as well as potentially leading to a change in material properties. Secondly, errors in calibration and weight measurement of the magnets could have contributed to the error in the calculation of the spring stiffness. The variation in spring stiffness has resulted in a slight alteration in the current vs displacement behavior. As the stiffness value is lower than the estimated value, the spring will displace more for the same current applied.

To decrease the error in spring stiffness, a few measures can be taken. Firstly, adjusting the laser cutting settings could help to reduce the thermal stresses induced during fabrication. This could result in more accurate and consistent spring stiffness. Secondly, alternative fabrication methods such as photochemical machining or waterjet cutting may be considered, which may not have as significant an impact on the material properties as laser cutting. Additionally, careful calibration and measurement of the weights used during experimentation can help to minimize the potential sources of error in determining the spring stiffness. Furthermore, the results obtained from these experiments can be used to refine the theoretical models used for predicting spring stiffness. The experimental data can be incorporated into the models to improve their accuracy, and further simulations can be performed to identify any other factors that may be affecting the spring stiffness. This iterative process of experimentation and simulation can lead to a better understanding of the system and more precise control over its behavior.

5.2 Current vs Displacement

This experiment was performed to characterize the actuator behavior (i.e., obtain the current vs. displacement graph). The coupling mechanism was actuated for different values of current ranging from 30 - 80 mA. At 80 mA, the actuator experiences its maximum displacement, which means that the magnet has been fully displaced and has moved into the coil. Additionally, the magnet base will be in contact with the coil, indicating that the actuator has reached its maximum displacement limit. Three trials were conducted each trial starting from a different current actuation. The displacement achieved was plotted in Fig. 5.3 which depicts an almost linear behavior. The maximum deflection achieved was 1.1 mm.

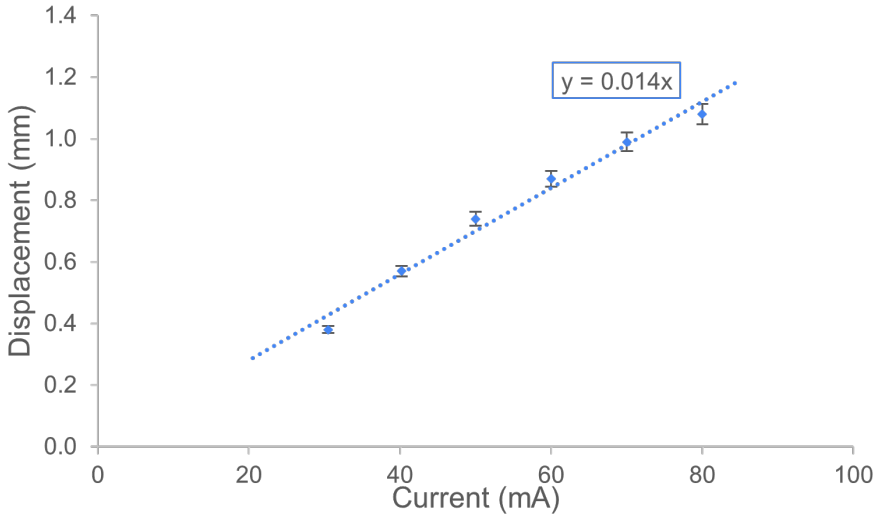

Figure 5.3: Current vs Displacement graph of the actuator. The graph depicts a linear behavior.

To improve the performance of the actuator, various measures can be taken. Firstly, the coil's winding quality is a critical component of the actuator, and a

more uniform winding can increase overall performance. One option is to use a machine to wind the coil, which can ensure greater consistency in the magnetic field. Additionally, adding more turns to the coil can increase its magnetic field strength and result in a stronger actuator. This can be achieved by either using a thinner wire or increasing the size of the coil. However, it's important to note that decreasing the wire diameter can increase resistance and lead to high heat loss, so an extensive analysis of current consumption and heat loss is necessary to determine the optimal wire diameter and the number of turns. By taking these steps, the performance of the actuator can be significantly improved.

5.3 Docking Demonstration

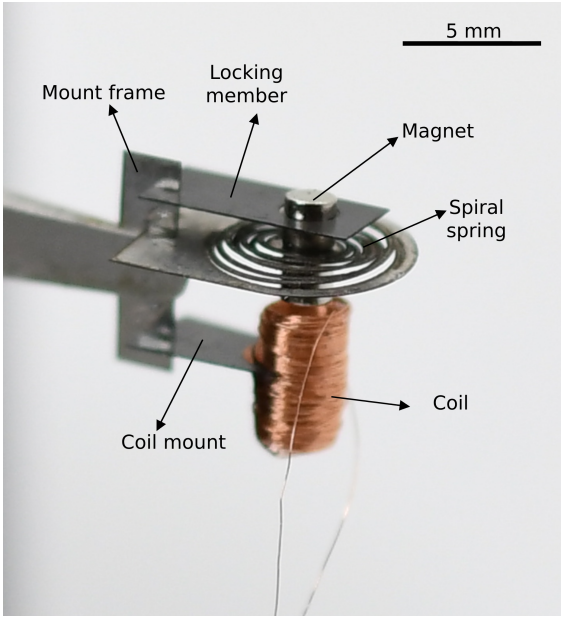

Figure 5.4: Different parts of the mechanism

The design of the mechanism has been successfully implemented, with the coil mounted on a cantilever beam made of carbon laminate. The mechanism consists of various components that have been assembled and connected on a

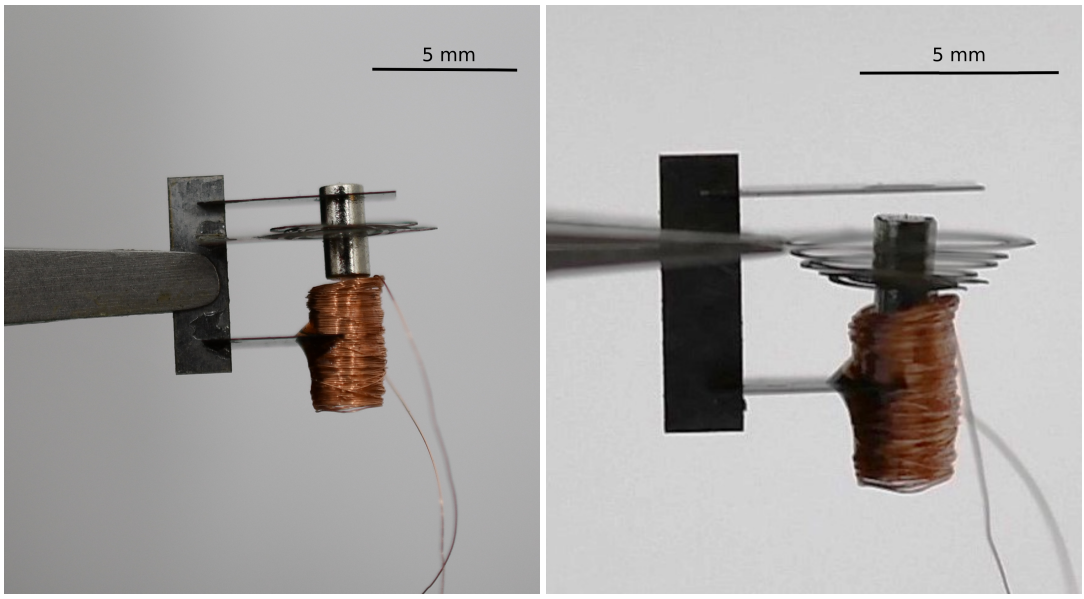

(a) (b)

Figure 5.5: The mechanism at different levels of actuation (a) The mechanism at zero actuation. (b) The mechanism at full actuation. At full actuation, the magnet has displaced 1.1 mm.

steel mount frame using slots and glue, as illustrated in Fig. 5.4. The mechanism's functionality at different levels of actuation is shown in Fig. 5.5, demonstrating the mechanism's ability to move the pin/magnet. Additionally, Fig. 5.6 displays snapshots of the manual docking process, where the locking counterpart approaches the mechanism, inserts into the clearance once actuated, and successfully docks after actuation is turned off. These results demonstrate the successful implementation of the mechanism and its ability to perform its intended function.

5.4 Loading Test

In this experiment, we aimed to measure the holding force of the coupling mechanism under normal loading conditions. To achieve this, we fabricated a female

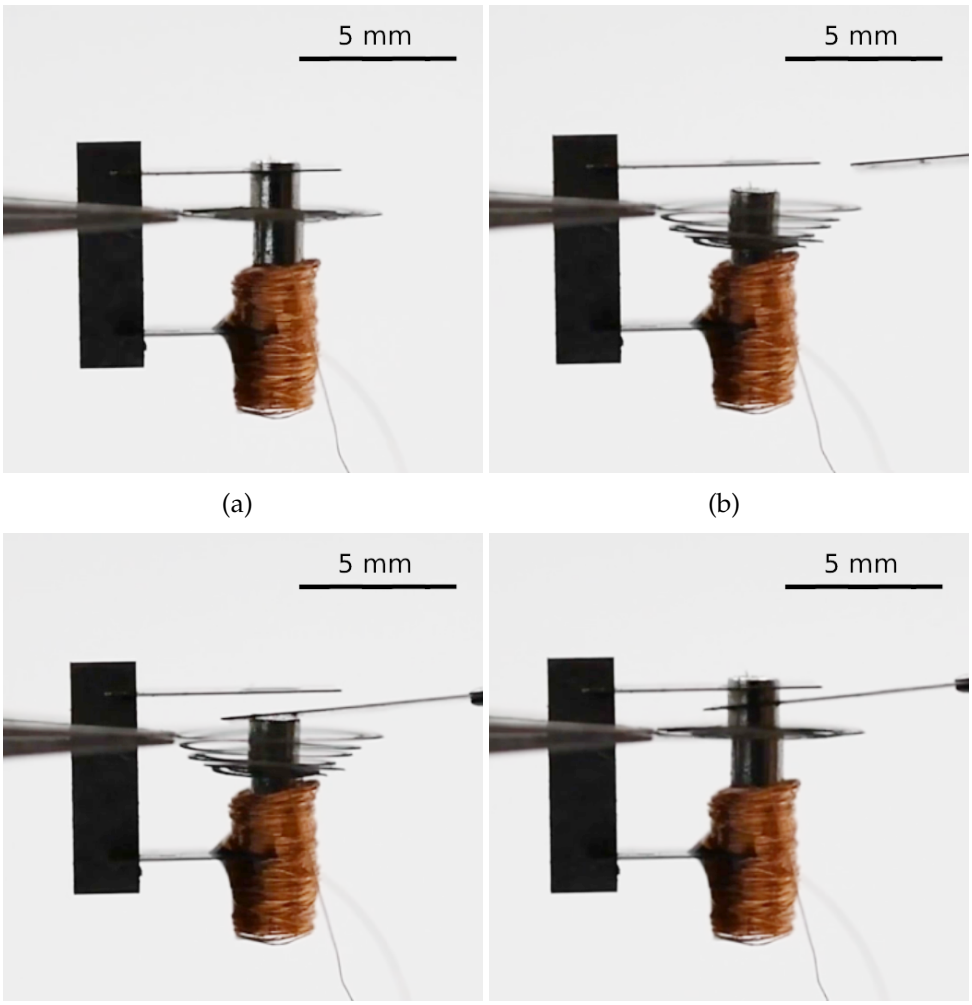

Figure 5.6: (a)-(d) Snapshots of the manual docking process between the mechanism and a locking counterpart.

part and used washers of known weights to apply a gradually increasing load. As the load increased, the magnet mount on the spiral spring rotated out of the plane, leading to a corresponding increase in the applied force. This process continued until the mechanism failed, indicated by the magnet rotating enough to cause the decoupling of the female part. We found that the maximum holding force of the mechanism was 75mN.

The coupling mechanism has the capacity to hold up to 7 gram-weight mi-

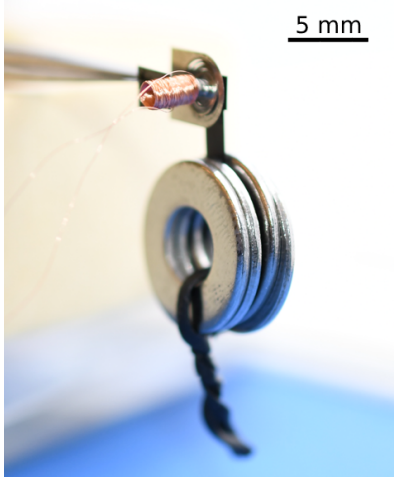

Figure 5.7: Normal loading test setup.

crorobots, allowing for the formation of chain-like structures. To increase the holding force, it is advisable to enhance the out-of-plane torsional stiffness of the planar spiral spring. This can be accomplished by selecting a material with a higher modulus of elasticity, which results in increased stiffness of the spring. Another alternative is to increase the thickness of the spring material, which can also lead to greater stiffness and an increase in the holding force. A thorough analysis should be conducted to determine the optimal approach to improving the out-of-plane torsional stiffness of the planar spiral spring.

CHAPTER 6

CONCLUSION AND FUTURE WORK

This work reports a new docking mechanism designed for a cm-scale ambulatory microrobot. This design can be adapted to other legged microrobots. This thesis explores a docking mechanism to introduce modularity for insect-scale legged robots, to our knowledge, the first of its kind. This enables microrobots to form chain-like structures which potentially increase the payload capacity, and traverse obstacles and gaps larger than their bodylength.

6.1 Future work

While the current work has presented a promising docking mechanism for introducing modularity in microrobotic systems, there are still several steps to be taken to achieve a fully autonomous modular robotics system. The docking mechanism serves as a critical component in enabling the creation of reconfigurable systems from smaller, simpler modules. However, there are several steps that need to be taken in order to implement this mechanism on a microrobot.

Integration

Integration of the docking mechanism onto a microrobot is an important step in realizing the full potential of modular microrobotics. One possible approach is to attach the mechanism to the microrobot through a custom-designed interface. The interface should ensure that the docking mechanism is firmly attached to the microrobot while still allowing it to move freely. The power and control

signals can be routed to the mechanism through wires or wireless communication, depending on the specific application requirements. Additionally, the docking mechanism may need to be modified to suit the specific needs of the microrobot, such as adjusting the size and shape of the spring or the magnet. Integration of the docking mechanism onto a microrobot will require careful design and testing to ensure that it operates reliably and does not interfere with the microrobot's functionality.

Mechanical testing

Extensive mechanical testing of the docking mechanism is necessary to determine the maximum holding forces that can be achieved. The current work has characterized the holding force of the coupling mechanism under normal loading conditions, but more rigorous testing is required to fully understand its capabilities. Testing under different loading conditions, such as lateral and torsional loading, can provide insight into the mechanism's robustness and ability to withstand different types of external forces. Additionally, long-term durability testing can be performed to ensure that the mechanism can maintain its holding force over an extended period of time. By conducting thorough mechanical testing, the performance limits of the docking mechanism can be determined and its reliability can be established, which is crucial for its successful integration into microrobotic systems.

Spring design

Future work can also explore the optimization of the ortho-planar spring design. While the current design provides the desired displacement, exploring other designs may yield even better results. Other parameters such as different materials, thicknesses, and geometries can be examined to improve spring performance. Additionally, more complex spring designs, such as those with multiple layers or curved shapes, can also be explored to achieve the desired displacement with greater accuracy and consistency. By improving the spring design, the overall performance of the actuator can be enhanced, leading to more reliable and efficient docking operations.

At-scale electronics

Future work also involves the at-scale electronics implementation of the docking mechanism. The current prototype uses an Arduino board and conventional integrated circuits (IC) to drive the actuator, however, at scale, smaller and efficient drivers will be required. One promising option is the DRV8837, a low-voltage motor driver with a small form factor (2 mm x 2 mm) and a wide operating range (0 V to 11 V). The DRV8837 can drive a single motor with up to 1 A of peak current and is designed for battery-powered applications. Due to its small size and low voltage operation, the DRV8837 is an ideal option for implementing the at-scale electronics of the docking mechanism.

Autonomous docking

Autonomous docking is an essential aspect of modularity in microrobots. To achieve autonomous docking, a sensing system needs to be incorporated into the docking mechanism. Kim et al., in [37] estimated distance using RF and used a Kalman Filter (KF) for estimating the position and heading angle. Wang et al., in [70] propose a novel arithmetic of centering alignment based on an ultrasonic sensor for self-reconfigurable robots JL-2. Won et al., [73] introduce a novel and robust autonomous docking mechanism that employs an Extended Kalman Filter (EKF) to calculate accurate distance and orientation data by utilizing inexpensive IR emitters, IR receivers, and encoders. However, these sensing systems are not feasible for cm-scale microrobots due to their size and power constraints. Therefore, alternative solutions such as intelligent mechanical design, such as incorporating tactile sensors, or using external sensing systems such as a camera or laser rangefinder may be necessary.

6.2 Conclusion

In conclusion, the development of a docking mechanism for cm-scale ambulatory microrobots opens up new possibilities for the design of modular and versatile robotic systems. The mechanism enables the formation of chain-like structures that can navigate unstructured environments. The research presented in this dissertation investigated various electromechanical docking and actuation methods, leading to the design of a suitable mechanism for cm-scale microrobots. However, there are still several challenges that need to be addressed to achieve a fully autonomous and functional microrobot system. These in-

clude the optimization of power consumption, extensive mechanical testing, at-scale electronics, and improvement of the docking mechanism. As a multidisciplinary effort, this research requires the expertise of a diverse group of researchers to overcome these challenges and unlock the potential of cm-scale ambulatory microrobots. In summary, the development of a docking mechanism for cm-scale microrobots represents a significant step toward the realization of autonomous microrobotic platforms for various applications.

APPENDIX A

PYTHON CODE

```
import numpy as np
import matplotlib.pyplot as plt

calibration  = 99

def lineseg_dist(p, a, b):

    # normalized tangent vector
    d = np.divide(b - a, np.linalg.norm(b - a))

    # signed parallel distance components
    s = np.dot(a - p, d)
    t = np.dot(p - b, d)

    # clamped parallel distance
    h = np.maximum.reduce([s, t, 0])

    # perpendicular distance component
    c = np.cross(p - a, d)

    return np.hypot(h, np.linalg.norm(c))

def get_xy(filename):
    image = plt.imread(filename)
    h = image.shape[0]
    w = image.shape[1]
    fig,ax = plt.subplots()
    ax.imshow(image)
```

```
    fig.suptitle('Click middle button to stop input')
    xy = fig.ginput(-1,timeout = 45,show_clicks = True)
    x, y = zip(*xy)
    p = np.array([x[-1],y[-1]])
    a = np.array([x[0],y[0]])
    b = np.array([x[1],y[1]])
    return p,a,b


if __name__=="__main__":
    d = np.empty((0,3))
    for i in range(7):
        p,a,b = get_xy(str(i) + '.jpg')
        dist1 = lineseg_dist(p,a,b) / calibration
        p,a,b = get_xy(str(i) + '-.jpg')
        dist2 = lineseg_dist(p,a,b) / calibration
        plt.close('all')
        dist = np.mean((dist1,dist2))
        print(f'{dist1 :0.3f} ,{dist2 :0.3f}')
        print(f'for case {i} delta is {dist : .3f}')
        d = np.concatenate((d,np.array([[i,dist1,dist2]])))

    np.savetxt("delta.csv", d, delimiter=",")
```

BIBLIOGRAPHY

[1] Improvement in car-couplings, April 29 1873. US Patent 138,405.

[2] Carl Anderson, Guy Theraulaz, and J-L Deneubourg. Self-assemblages in insect societies. *Insectes sociaux*, 49(2):99–110, 2002.

[3] José Baca, SGM Hossain, Prithviraj Dasgupta, Carl A Nelson, and Ayan Dutta. Modred: Hardware design and reconfiguration planning for a high dexterity modular self-reconfigurable robot for extra-terrestrial exploration. *Robotics and Autonomous Systems*, 62(7):1002–1015, 2014.

[4] Andrew T Baisch, Onur Ozcan, Benjamin Goldberg, Daniel Ithier, and Robert J Wood. High speed locomotion for a quadrupedal microrobot. *The International Journal of Robotics Research*, 33(8):1063–1082, 2014.

[5] Palak Bhushan and Claire J Tomlin. Milligram-scale micro aerial vehicle design for low-voltage operation. In *2018 IEEE/RSJ International Conference on Intelligent Robots and Systems (IROS)*, pages 1–9. IEEE, 2018.

[6] Palak Bhushan and Claire J Tomlin. Design of the first sub-milligram flapping wing aerial vehicle. In *2019 IEEE 32nd International Conference on Micro Electro Mechanical Systems (MEMS)*, pages 2–5. IEEE, 2019.

[7] Paul Birkmeyer, Kevin Peterson, and Ronald S Fearing. Dash: A dynamic 16g hexapedal robot. In *2009 IEEE/RSJ international conference on intelligent robots and systems*, pages 2683–2689. IEEE, 2009.

[8] Roger Darchen. techniques de construction chez apis mellifica. 1959.

[9] Jay Davey, Ngai Kwok, and Mark Yim. Emulating self-reconfigurable robots-design of the smores system. In *2012 IEEE/RSJ international conference on intelligent robots and systems*, pages 4464–4469. IEEE, 2012.

[10] Sébastien D de Rivaz, Benjamin Goldberg, Neel Doshi, Kaushik Jayaram, Jack Zhou, and Robert J Wood. Inverted and vertical climbing of a quadrupedal microrobot using electroadhesion. *Science Robotics*, 3(25):eaau3038, 2018.

[11] Don L DeVoe and Albert P Pisano. Modeling and optimal design of piezoelectric cantilever microactuators. *Journal of Microelectromechanical systems*, 6(3):266–270, 1997.

[12] Guoqiang Fu, Arianna Menciassi, and Paolo Dario. Development of a genderless and fail-safe connection system for autonomous modular robots. In *2011 IEEE International Conference on Robotics and Biomimetics*, pages 877–882. IEEE, 2011.

[13] Robert J Full and Michael S Tu. Mechanics of a rapid running insect: two-, four-and six-legged locomotion. *Journal of Experimental Biology*, 156(1):215–231, 1991.

[14] Kyle Gilpin, Ara Knaian, and Daniela Rus. Robot pebbles: One centimeter modules for programmable matter through self-disassembly. In *2010 IEEE International Conference on Robotics and Automation*, pages 2485–2492. IEEE, 2010.

[15] Seth Goldstein. Modular robots. *IEEE Robotics & Automation Magazine*, 14(4):43–52, December 2007.

[16] Moritz A Graule, Pakpong Chirarattananon, Sawyer B Fuller, Noah T Jafferis, Kevin Y Ma, Matthew Spenko, Roy Kornbluh, and Robert J Wood. Perching and takeoff of a robotic insect on overhangs using switchable electrostatic adhesion. *Science*, 352(6288):978–982, 2016.

[17] Shuxiang Guo, Toshio Fukuda, Norihiko Kato, and Keisuke Oguro. Development of underwater microrobot using icpf actuator. In *Proceedings. 1998 IEEE International Conference on Robotics and Automation (Cat. No. 98CH36146)*, volume 2, pages 1829–1834. IEEE, 1998.

[18] Shuxiang Guo, Seiji Hata, Koichi Sugumoto, Toshio Fukuda, and Keisuke Oguro. Development of a new type of capsule micropump. In *Proceedings 1999 IEEE International Conference on Robotics and Automation (Cat. No. 99CH36288C)*, volume 3, pages 2171–2176. IEEE, 1999.

[19] Berthold K H lldobler and Edward O Wilson. Weaver ants. *Scientific American*, 237(6):146–155, 1977.

[20] Hassan H Hariri, Leonardus A Prasetya, Shaohui Foong, Gim Song Soh, Kevin N Otto, and Kristin L Wood. A tether-less legged piezoelectric miniature robot using bounding gait locomotion for bidirectional motion. In *2016 IEEE International Conference on Robotics and Automation (ICRA)*, pages 4743–4749. IEEE, 2016.

[21] M Hisanaga, T Kurahashi, M Kodera, and T Hattori. Fabrication of a 4.8

millimeter long microcar. In *Proc. Second Int. Symp. on Micro Machine and Human Science*, pages 43–46, 1991.

[22] Katie L Hoffman and Robert J Wood. Myriapod-like ambulation of a segmented microrobot. *Autonomous Robots*, 31(1):103–114, 2011.

[23] Bert Hölldobler and Edward O Wilson. The evolution of communal nest-weaving in ants: Steps that may have led to a complicated form of cooperation in weaver ants can be inferred from less advanced behavior in other species. *American Scientist*, 71(5):490–499, 1983.

[24] Aaron M Hoover, Samuel Burden, Xiao-Yu Fu, S Shankar Sastry, and Ronald S Fearing. Bio-inspired design and dynamic maneuverability of a minimally actuated six-legged robot. In *2010 3rd IEEE RAS & EMBS International Conference on Biomedical Robotics and Biomechatronics*, pages 869–876. IEEE, 2010.

[25] Aaron M Hoover, Erik Steltz, and Ronald S Fearing. Roach: An autonomous 2.4 g crawling hexapod robot. In *2008 IEEE/RSJ international conference on intelligent robots and systems*, pages 26–33. IEEE, 2008.

[26] Jie Hu, Si Chen, and Le Wang. A new insect-scale piezoelectric robot with asymmetric structure. *IEEE Transactions on Industrial Electronics*, 2022.

[27] Takaharu Idogaki, Hitoshi Kanayama, Nobuyuki Ohya, Harumi Suzuki, and Tadashi Hattori. Characteristics of piezoelectric locomotive mechanism for an in-pipe micro inspection machine. In *MHS'95. Proceedings of the Sixth International Symposium on Micro Machine and Human Science*, pages 193–198. IEEE, 1995.

[28] Takahiro Ito, Takuto Ogushi, and Teru Hayashi. Impulse-driven capsule by coil-induced magnetic field implementation. *Mechanism and Machine theory*, 45(11):1642–1650, 2010.

[29] Klaus Jaffe. Surfing ants. *Florida Entomologist*, pages 182–183, 1993.

[30] Kaushik Jayaram, Jennifer Shum, Samantha Castellanos, E Farrell Helbling, and Robert J Wood. Scaling down an insect-size microrobot, hamr-vi into hamr-jr. In *2020 IEEE International Conference on Robotics and Automation (ICRA)*, pages 10305–10311. IEEE, 2020.

[31] X Jia, M Frenger, Z Chen, William R Hamel, and Mingjun Zhang. An alliga-

tor inspired modular robot. In *2015 IEEE International Conference on Robotics and Automation (ICRA)*, pages 1949–1954. IEEE, 2015.

[32] Gangyuan Jing, Tarik Tosun, Mark Yim, and Hadas Kress-Gazit. An end-to-end system for accomplishing tasks with modular robots. In *Robotics: Science and systems*, volume 2, page 7, 2016.

[33] Gangyuan Jing, Tarik Tosun, Mark Yim, and Hadas Kress-Gazit. Accomplishing high-level tasks with modular robots. *Autonomous Robots*, 42(7):1337–1354, 2018.

[34] RE Joerres. Springs.(retroactive coverage). *McGraw-Hill, Inc., Standard Handbook of Machine Design,*, page 24, 1986.

[35] Mustafa Emre Karagozler, Jason D Campbell, Gary K Fedder, Seth Copen Goldstein, Michael Philetus Weller, and Byung Woo Yoon. Electrostatic latching for inter-module adhesion, power transfer, and communication in modular robots. In *2007 IEEE/RSJ International Conference on Intelligent Robots and Systems*, pages 2779–2786. IEEE, 2007.

[36] Byungkyu Kim, Jaewook Ryu, Younkoo Jeong, Younghun Tak, Byungmok Kim, and Jong-Oh Park. A ciliary based 8-legged walking micro robot using cast ipmc actuators. In *2003 IEEE International Conference on Robotics and Automation (Cat. No. 03CH37422)*, volume 3, pages 2940–2945. IEEE, 2003.

[37] Myungsik Kim, Nak Young Chong, and Wonpil Yu. Robust doa estimation and target docking for mobile robots. *Intelligent Service Robotics*, 2:41–51, 2009.

[38] Je-Sung Koh and Kyu-Jin Cho. Omegabot: Biomimetic inchworm robot using sma coil actuator and smart composite microstructures (scm). In *2009 IEEE international conference on robotics and biomimetics (ROBIO)*, pages 1154–1159. IEEE, 2009.

[39] Keith Kotay, Daniela Rus, Marsette Vona, and Craig McGray. The self-reconfiguring robotic molecule. In *Proceedings. 1998 IEEE International Conference on Robotics and Automation (Cat. No. 98CH36146)*, volume 1, pages 424–431. IEEE, 1998.

[40] Haruhisa Kurokawa, Akiya Kamimura, Eiichi Yoshida, Kohji Tomita, Shigeru Kokaji, and Satoshi Murata. M-tran ii: metamorphosis from a

four-legged walker to a caterpillar. In *Proceedings 2003 IEEE/RSJ International Conference on Intelligent Robots and Systems (IROS 2003)(Cat. No. 03CH37453)*, volume 3, pages 2454–2459. IEEE, 2003.

[41] Haruhisa Kurokawa, Kohji Tomita, Akiya Kamimura, Shigeru Kokaji, Takashi Hasuo, and Satoshi Murata. Distributed self-reconfiguration of m-tran iii modular robotic system. *The International Journal of Robotics Research*, 27(3-4):373–386, 2008.

[42] Dongwoo Lee, Sinbae Kim, Yong-Lae Park, and Robert J Wood. Design of centimeter-scale inchworm robots with bidirectional claws. In *2011 IEEE International Conference on Robotics and Automation*, pages 3197–3204. IEEE, 2011.

[43] Jens Liedke, Rene Matthias, Lutz Winkler, and Heinz Wörn. The collective self-reconfigurable modular organism (cosmo). In *2013 IEEE/ASME International Conference on Advanced Intelligent Mechatronics*, pages 1–6. IEEE, 2013.

[44] Chao Liu, Qian Lin, Hyun Kim, and Mark Yim. Parallel self-assembly with smores-ep, a modular robot. In *2020 International Conference on Robotics and Automation (ICRA), accepted*, 2020.

[45] Haiwei Lu, Jianguo Zhu, Zhiwei Lin, and Youguang Guo. An inchworm mobile robot using electromagnetic linear actuator. *Mechatronics*, 19(7):1116–1125, 2009.

[46] Ronald Lumia and Mohsen Shahinpoor. Microgripper design using electroactive polymers. In *Smart Structures and Materials 1999: Electroactive Polymer Actuators and Devices*, volume 3669, pages 322–329. SPIE, 1999.

[47] Sylvain Martel. Fundamental principles and issues of high-speed piezoactuated three-legged motion for miniature robots designed for nanometer-scale operations. *The International Journal of Robotics Research*, 24(7):575–588, 2005.

[48] Arianna Menciassi, Dino Accoto, Samuele Gorini, and Paolo Dario. Development of a biomimetic miniature robotic crawler. *Autonomous Robots*, 21(2):155–163, 2006.

[49] Satoshi Murata, Eiichi Yoshida, Akiya Kamimura, Haruhisa Kurokawa, Kohji Tomita, and Shigeru Kokaji. M-tran: Self-reconfigurable modular robotic system. *IEEE/ASME transactions on mechatronics*, 7(4):431–441, 2002.

[50] Devin M Neal and H Harry Asada. Bipolar piezoelectric buckling actuators. *IEEE/ASME Transactions on Mechatronics*, 19(1):9–19, 2012.

[51] Jonas Neubert, Arne Rost, and Hod Lipson. Self-soldering connectors for modular robots. *IEEE Transactions on Robotics*, 30(6):1344–1357, 2014.

[52] QS Nguyen, S Heo, HC Park, and D Byun. Performance evaluation of an improved fish robot actuated by piezoceramic actuators. *Smart Materials and Structures*, 19(3):035030, 2010.

[53] M Ono, I Okada, and M Sasaki. Heat production by balling in the japanese honeybee, apis cerana japonica as a defensive behavior against the hornet, vespa simillima xanthoptera (hymenoptera: Vespidae). *Experientia*, 43:1031–1034, 1987.

[54] Yasemin Ozkan-Aydin and Daniel I Goldman. Self-reconfigurable multilegged robot swarms collectively accomplish challenging terradynamic tasks. *Science Robotics*, 6(56):eabf1628, 2021.

[55] Jan Peirs, Dominiek Reynaerts, and Hendrik Van Brussel. Scale effects and thermal considerations for micro-actuators. In *Proceedings. 1998 IEEE International Conference on Robotics and Automation (Cat. No. 98CH36146)*, volume 2, pages 1516–1521. IEEE, 1998.

[56] Andrew O Pullin, Nicholas J Kohut, David Zarrouk, and Ronald S Fearing. Dynamic turning of 13 cm robot comparing tail and differential drive. In *2012 IEEE International Conference on Robotics and Automation*, pages 5086–5093. IEEE, 2012.

[57] Shannon A Rios, Andrew J Fleming, and Yuen Kuan Yong. Miniature resonant ambulatory robot. *IEEE Robotics and Automation Letters*, 2(1):337–343, 2016.

[58] Jesse A Roll, Bo Cheng, and Xinyan Deng. An electromagnetic actuator for high-frequency flapping-wing microair vehicles. *IEEE Transactions on Robotics*, 31(2):400–414, 2015.

[59] John W Romanishin, Kyle Gilpin, and Daniela Rus. M-blocks: Momentum-driven, magnetic modular robots. In *2013 IEEE/RSJ International Conference on Intelligent Robots and Systems*, pages 4288–4295. IEEE, 2013.

[60] Ranjana Sahai, Srinath Avadhanula, Richard Groff, Erik Steltz, Robert

Wood, and Ronald S Fearing. Towards a 3g crawling robot through the integration of microrobot technologies. In *Proceedings 2006 IEEE International Conference on Robotics and Automation, 2006. ICRA 2006.*, pages 296–302. IEEE, 2006.

[61] Theodore Christian Schneirla. Army ants: a study in social organization. 1971.

[62] Bu Hyun Shin, Seung-Wook Choi, Young-Bong Bang, and Seung-Yop Lee. An earthworm-like actuator using segmented solenoids. *Smart materials and structures*, 20(10):105020, 2011.

[63] Alexander Sproewitz, Aude Billard, Pierre Dillenbourg, and Auke Jan Ijspeert. Roombots-mechanical design of self-reconfiguring modular robots for adaptive furniture. In *2009 IEEE international conference on robotics and automation*, pages 4259–4264. IEEE, 2009.

[64] K Stoy, A Lyder, R Franco, and et al. Genderless connection mechanism for modular robots introducing torque transmission between modules. In *IEEE International Conference on Robotics and Automation Workshop on Modular Robots: State of the Art*, pages 77–81, 2010.

[65] Kasper Støy, David Brandt, and David J Christensen. *Self-reconfigurable robots*. MIT Press Cambridge, 2010.

[66] Satoshi Tadokoro, Takahiko Murakami, Satoshi Fuji, Ryu Kanno, Motofumi Hattori, Toshi Takamori, and Keisuke Oguro. An elliptic friction drive element using an icpf actuator. *IEEE Control Systems Magazine*, 17(3):60–68, 1997.

[67] James Torres and H Harry Asada. High-gain, high transmissibility pzt displacement amplification using a rolling-contact buckling mechanism and preload compensation springs. *IEEE Transactions on Robotics*, 30(4):781–791, 2014.

[68] Tarik Tosun, Jay Davey, Chao Liu, and Mark Yim. Design and characterization of the ep-face connector. In *2016 IEEE/RSJ International Conference on Intelligent Robots and Systems (IROS)*, pages 45–51. IEEE, 2016.

[69] Jun Ueda, Thomas W Secord, and H Harry Asada. Large effective-strain piezoelectric actuators using nested cellular architecture with exponential strain amplification mechanisms. *IEEE/ASME transactions on mechatronics*, 15(5):770–782, 2009.

[70] Wei Wang, Zongliang Li, Wenpeng Yu, and Jianwei Zhang. An autonomous docking method based on ultrasonic sensors for self-reconfigurable mobile robot. In *2009 IEEE International Conference on Robotics and Biomimetics (ROBIO)*, pages 1744–1749. IEEE, 2009.

[71] Zhenlong Wang, Guanrong Hang, Jian Li, Yangwei Wang, and Kai Xiao. A micro-robot fish with embedded sma wire actuated flexible biomimetic fin. *Sensors and Actuators A: Physical*, 144(2):354–360, 2008.

[72] Kevin C Wolfe, Matthew S Moses, Michael DM Kutzer, and Gregory S Chirikjian. M 3 express: a low-cost independently-mobile reconfigurable modular robot. In *2012 IEEE International Conference on Robotics and Automation*, pages 2704–2710. IEEE, 2012.

[73] Peter Won, Mohammad Biglarbegian, and William Melek. Development of an effective docking system for modular mobile self-reconfigurable robots using extended kalman filter and particle filter. *Robotics*, 4(1):25–49, 2015.

[74] Robert J Wood. The first takeoff of a biologically inspired at-scale robotic insect. *IEEE transactions on robotics*, 24(2):341–347, 2008.

[75] Sha Yi, Zeynep Temel, and Katia Sycara. Puzzlebots: physical coupling of robot swarms. In *2021 IEEE International Conference on Robotics and Automation (ICRA)*, pages 8742–8748. IEEE, 2021.

[76] Mark Yim, Ying Zhang, Kimon Roufas, David Duff, and Craig Eldershaw. Connecting and disconnecting for chain self-reconfiguration with polybot. *IEEE/ASME Transactions on mechatronics*, 7(4):442–451, 2002.

[77] Yang Zou, Weiping Zhang, and Zheng Zhang. Liftoff of an electromagnetically driven insect-inspired flapping-wing robot. *IEEE Transactions on Robotics*, 32(5):1285–1289, 2016.